Weierstraß-Institut

für Angewandte Analysis und Stochastik

Leibniz-Institut im Forschungsverbund Berlin e. V.

Preprint ISSN 0946 – 8633

The factorization method for inverse elastic scattering from periodic structures

Guanghui Hu[1], Yulong Lu[2], Bo Zhang[3]

submitted: April 29, 2013

[1] Weierstrass Institute
Mohrenstr. 39
10117 Berlin
Germany
E-Mail: guanghui.hu@wias-berlin.de

[2] Institute of Applied Mathematics
AMSS
Chinese Academy of Sciences
Beijing 100190
China
E-Mail: luyulong@amss.ac.cn

[3] LSEC and Institute of Applied Mathematics
AMSS
Chinese Academy of Sciences
Beijing 100190
China
E-Mail: b.zhang@amt.ac.cn

No. 1782

Berlin 2013

2010 *Mathematics Subject Classification.* 35R30, 74B05, 78A46, 35Q93.

Key words and phrases. Inverse elastic scattering, factorization method, Dirichlet boundary condition, Navier equation, uniqueness.

The first author (GH) gratefully acknowledges the support by the German Research Foundation (DFG) under Grant No. HU 2111/1-1. The work of the third author (BZ) is supported by the National Natural Science Foundation of China under grant No. 11071244.

Edited by
Weierstraß-Institut für Angewandte Analysis und Stochastik (WIAS)
Leibniz-Institut im Forschungsverbund Berlin e. V.
Mohrenstraße 39
10117 Berlin
Germany

Fax: +49 30 20372-303
E-Mail: preprint@wias-berlin.de
World Wide Web: http://www.wias-berlin.de/

Abstract

This paper is concerned with the inverse scattering of time-harmonic elastic waves from rigid periodic structures. We establish the factorization method to identify an unknown grating surface from knowledge of the scattered compressional or shear waves measured on a line above the scattering surface. Near-field operators are factorized by selecting appropriate incident waves derived from quasi-periodic half-space Green's tensor to the Navier equation. The factorization method gives rise to a uniqueness result for the inverse scattering problem by utilizing only the compressional or shear components of the scattered field corresponding to all quasi-periodic incident plane waves with a common phase-shift. A number of computational examples are provided to show the accuracy of the inversion algorithms, with an emphasis placed on comparing reconstructions from the scattered near-field and those from its compressional and shear components.

1 Introduction

The inverse scattering problem of recovering an unknown grating profile (periodic structure) from the scattered field is of great importance, e.g., in diffractive optics, quality control and design of diffractive elements with prescribed far-field patterns [7, 32]. Consequently, there is a vast literature on the reconstruction of grating interfaces modeled by the Maxwell equations or the two-dimensional Helmholtz equation (see e.g. [1, 5, 6, 20, 22, 19, 16, 28, 30, 33, 34]). The inverse elastic scattering by periodic structures has also a wide field of applications, particularly in geophysics, seismology and nondestructive testing. For instance, identifying fractures in sedimentary rocks can have significant impact on the production of underground gas and liquids by employing controlled explosions. The sedimentary rock under consideration can be regarded as a homogeneous transversely isotropic elastic medium with periodic vertical fractures that can be extended to infinity in one of the horizontal directions. Using an elastic plane wave as an incoming source, we thus get an inverse problem of shape identification from the knowledge of near-field data measured above the periodic structure; see [29]. Analogous inverse problems also arise from using transient elastic waves to measure the elastic properties or to detect flaws and cracks in concrete structures. Moreover, the problem of elastic pulse transmission and reflection through the earth is fundamental to both the investigation of earthquakes and the utility of seismic waves in search for oil and ore bodies ([17, 18]).

This paper is concerned with the inverse elastic diffraction problem (IP) of recovering a two-dimensional rigid grating profile from scattered near-field, which can be regarded as a simple model problem in elasticity. The direct scattering problem (DP) can be formulated as a Dirichlet boundary value problem for the time-harmonic Navier equation in the unbounded domain above the scattering surface. We refer to [3, 4, 12, 13, 15] or Section 2 of this paper concerning existence and uniqueness results to the forward scattering. We shall establish the factorization method for (IP), generalizing the inversion algorithms in the acoustic scattering from bounded obstacles [6, 11, 26, 24] and diffraction gratings [6, 5, 28] to the current situation. The factorization method was firstly put forward by Kirsch [24] to reconstruct bounded obstacles from spectral data of the far-field patterns. It requires neither computation of direct solutions nor initial guesses, and provides a sufficient and necessary condition for precisely characterizing the shape of unknown scatterers. We refer to [25, 30, 31] for the factorization method applied to inverse electromagnetic medium scattering from bounded obstacles and diffraction gratings. Schiffer's uniqueness theorem for (IP) was already justified in [10]. It was proved that a smooth grating surface (C^2) can be uniquely determined from incident pressure waves for one incident angle and an interval of wave numbers. Furthermore, a finite set of wave numbers is enough if a priori information about the height of the grating curve is known. This extends the periodic version of Schiffer's theorem by Hettlich and Kirsch (see [20]) to the case of inverse elastic diffraction problems. The application of the Kirsch-Kress optimization scheme to (IP) with one or several incident elastic plane waves can be found in [14].

Compared to the diffraction of acoustic waves, the elastic scattering is more complicated in view of the coexistence of compressional (also called longitudinal or dilatational) waves and shear (also called transverse or distortional) waves that propagate at different speeds. We divide our inverse problems into two classes, based on the phase-shifts of the incident elastic plane waves for a fixed incident angle. For each class, we study inverse problem by utilizing scattered compressional waves, shear waves or the entire scattered near-field. As a corollary, we obtain a uniqueness result using only the information of the scattered compressional or shear waves corresponding to all incident elastic plane waves with a common phase-shift. Such a result is in analogy with the one in [21] for bounded rigid obstacles using only compressional or shear waves.

Inspired by the existing factorization methods for diffraction gratings [5, 28] as well as for bounded obstacle scattering in a half-space [26, Chapter 2.6], we choose two admissible sets of incident waves based on the form of the quasi-periodic elastic Green's tensor in a half-plane. Such a Green's tensor is derived from the general (non-quasi-periodic) half-plane Green's function (see [4]) through Poisson's formula. The admissible sets of incident waves enable us to factorize the near-field operators in a standard way. To apply appropriate range identities, we investigate properties of the middle operator for small frequencies; see Remark 4.12. This differs from the factorization method established in [5, 28], where the role of the positive part of the middle operator is played by a single layer operator whose kernel is the quasi-periodic fundamental solution to the Helmholtz equation with the wave number $k = i$ or $k = 0$. The injectivity of the middle operator is justified under the assumption that the frequency of the incidence waves is not the quasi-periodic Dirichlet eigenvalue of the Lam$\acute{e}$ operator over a periodic strip.

The paper is organized as follows. In Section 2, we formulate the direct and inverse elastic scattering problems for diffraction gratings and collect some solvability results for the forward problem. Section 3 is devoted to describing the half-space quasi-periodic Green's tensor and two admissible sets of incident elastic waves with distinct phase-shifts. In Section 4 we provide a theoretical justification of the factorization method, following the spirit of [5, 21]. Numerical experiments are reported in Section 5 to test validity and stability of the factorization method, with an emphasis placed on comparing reconstructions from utilizing the scattered near-field and those from its compressional and shear components.

2 Direct and inverse diffraction problems

Let the diffraction grating profile be given by the graph Λ of a C^2-smooth 2π-periodic function f lying above the x_1-axis, i.e., $\Lambda = \{x_2 = f(x_1) > 0, x_1 \in \mathbb{R}\}$. Denote by Ω_Λ the unbounded region above Λ, and for simplicity assume that Ω_Λ is occupied by a linear isotropic and homogeneous elastic material with mass density one. Suppose that an incident pressure wave (with the incident angle $\theta \in (-\pi/2, \pi/2)$) given by

$$u_p^{in} = \hat{\theta} \exp(ik_p x \cdot \hat{\theta}), \qquad \hat{\theta} := (\sin\theta, -\cos\theta)^T \tag{1}$$

is incident on Λ from the region above. Here, $k_p := \omega/\sqrt{2\mu+\lambda}$ is the compressional wave number, λ and μ denote the Lamé constants satisfying $\mu > 0$ and $\lambda + \mu > 0$, $\omega > 0$ is the angular frequency of the harmonic motion, and the symbol $(\cdot)^T$ stands for the transpose of a vector in $\mathbb{R}^2$. The shear wave number is defined as $k_s := \omega/\sqrt{\mu}$. The direct problem for pressure wave incidence aims to find the scattered field $u^{sc} \in H^1_{loc}(\Omega_\Lambda)^2$ such that

$$\begin{aligned} (\Delta^* + \omega^2)\, u^{sc} &= 0 \quad \text{in} \quad \Omega_\Lambda, \quad \Delta^* := \mu\Delta + (\lambda+\mu)\, \mathrm{grad}\,\mathrm{div}\,, \\ u^{sc} &= -u_p^{in} \quad \text{on} \quad \Lambda. \end{aligned} \tag{2}$$

Recall that a function u is called quasi-periodic with phase-shift α (or α-quasi-periodic) if

$$u(x_1 + 2\pi, x_2) = \exp(2i\alpha\pi)\, u(x_1, x_2)\,, \quad (x_1, x_2) \in \Omega_\Lambda \tag{3}$$

Obviously, the incident pressure wave u_p^{in} is α-quasi-periodic with $\alpha = k_p \sin\theta$ over the periodic domain Ω_Λ. If the scattered field u^{sc} is also supposed to be quasi-periodic with the same phase-shift as the incident wave, then problem (2) admits a unique solution that satisfies the outgoing Rayleigh expansion

$$u^{sc}(x) = \sum_{n\in\mathbb{Z}} \left\{ A_{p,n} W_{p,n} \begin{pmatrix} \alpha_n \\ \beta_n \end{pmatrix} e^{i\alpha_n x_1 + i\beta_n x_2} + A_{s,n} W_{s,n} \begin{pmatrix} \gamma_n \\ -\alpha_n \end{pmatrix} e^{i\alpha_n x_1 + i\gamma_n x_2} \right\} \tag{4}$$

for $x_2 > h \geq \Lambda^+ := \max_{(x_1,x_2)\in\Lambda} x_2$. Here, the constants $A_{p,n},\ A_{s,n} \in \mathbb{C}$ are called the Rayleigh coefficients, the weights $W_{p,n}$ and $W_{s,n}$ are defined by

$$W_{p,n} := \begin{cases} 1, & \text{if} \quad |\alpha_n| < k_p\,, \\ \exp(-i\beta_n h), & \text{if} \quad |\alpha_n| \geq k_p\,, \end{cases} \qquad W_{s,n} := \begin{cases} 1, & \text{if} \quad |\alpha_n| < k_s\,, \\ \exp(-i\gamma_n h), & \text{if} \quad |\alpha_n| \geq k_s \end{cases} \tag{5}$$

and

$$\alpha_n := \alpha + n\,, \quad \beta_n = \beta_n(\theta) := \begin{cases} \sqrt{k_p^2 - \alpha_n^2} & \text{if} \quad |\alpha_n| \leq k_p\,, \\ i\,\sqrt{\alpha_n^2 - k_p^2} & \text{if} \quad |\alpha_n| > k_p. \end{cases} \tag{6}$$

The parameter $\gamma_n := \gamma_n(\theta)$ is defined similarly as β_n with k_p replaced by k_s. Concerning the proof of uniqueness and existence, we refer to [3] via integral equation methods for smooth (C^2) grating profiles and to [12, 13] where the variational approach is applied to case of general Lipschitz graphs in $\mathbb{R}^n$ ($n = 2, 3$). It is recently proved in [15] that such an α-quasiperiodic solution is the unique solution to (2) in the weighted Sobolev space

$$H^1_\varrho(S_h) := \{u :\ u = (1 + x_1^2)^{-\varrho/2} v,\ v \in H^1(S_h)\}\,, \qquad S_h := \Omega_\Lambda \backslash \{x = (x_1, x_2) : x_2 > h\}$$

for every $h > \Lambda^+$ and $-1 < \varrho < -1/2$. This implies that non-quasi-periodic or other α'-quasi-periodic ($\alpha' \neq k_p \sin\theta$) solutions to (2) does not exist in the space $H^1_\varrho(S_h)$. These solvability results in periodic structures extend those in acoustics (see [23, 8, 9]) to the case of elasticity. Moreover, they remain valid for a large class of quasi-periodic incident elastic waves as considered in the subsequent sections of this paper, provided the scattering surface is given by the graph of a periodic function. For non-graph grating profiles, existence of solutions to the problem (1)-(2) can be proved by applying the Fredholm alternative (see [12, 13]).

Since β_n and γ_n are real for at most a finite number of indices $n \in \mathbb{Z}$, only a finite number of plane waves in (4) propagate into the far field, with the remaining evanescent waves (or surface waves) decaying exponentially as $x_2 \to +\infty$. The above expansion converges uniformly with all derivatives in the half-plane $\{x \in \mathbb{R}^2 : x_2 \geq h\}$ and the Rayleigh coefficients $\{A_{p,n}\}_{n\in\mathbb{Z}}, \{A_{s,n}\}_{n\in\mathbb{Z}} \in \ell^2$. The scattered field can be decomposed into its compressional and shear parts,

$$u^{sc} = u_p^{sc} + u_s^{sc}, \quad u_p^{sc} := -1/k_p^2 \,\mathrm{grad}\,\mathrm{div}\, u^{sc}, \quad u_s^{sc} := 1/k_s^2 \,\overrightarrow{\mathrm{curl}}\,\mathrm{curl}\, u^{sc}$$

where $\mathrm{curl}\, u := \partial_1 u_2 - \partial_2 u_1$ for a vector function $u = (u_1, u_2)^T$ and $\overrightarrow{\mathrm{curl}}\, w = (\partial_2 w, -\partial_1 w)^T$ for a scalar function w. Particularly, the P- and S-waves admit respectively the expansions

$$\begin{aligned} u_p^{sc} &:= \sum_{n\in\mathbb{Z}} \left[A_{p,n}\, W_{p,n}\, (\alpha_n, \beta_n)^T \exp(i\alpha_n x_1 + i\beta_n x_2)\right], \\ u_s^{sc} &:= \sum_{n\in\mathbb{Z}} \left[A_{s,n}\, W_{s,n}\, (\gamma_n, -\alpha_n)^T \exp(i\alpha_n x_1 + i\gamma_n x_2)\right] \end{aligned} \tag{7}$$

for $x_2 > h$, which satisfy the equations

$$(\Delta + k_p^2) u_p^{sc} = 0, \quad \mathrm{curl}\, u_p^{sc} = 0, \quad (\Delta + k_s^2) u_s^{sc} = 0, \quad \mathrm{div}\, u_s^{sc} = 0 \quad \text{in} \quad \Omega_\Lambda$$

The uniqueness and existence results for a pressure wave can all be extended to an incident shear wave u_s^{in} of the form

$$u_s^{in} = \hat{\theta}^\perp \exp(ik_s \hat{\theta}), \quad \hat{\theta} := (\sin\theta, -\cos\theta)^\top, \; \hat{\theta}^\perp := (\cos\theta, \sin\theta)^\top \tag{8}$$

which is $k_s \sin\theta$-quasi-periodic. Note that, the phase-shift of the (unique) scattered field corresponding to (8) is $\alpha = k_s \sin\theta$, which differs from the case of P-wave incidence given in (1).

In this paper we are interested in the inverse problem of identifying an unknown rigid scattering surface Λ from knowledge of the scattered near field measured on a line above Λ. We always assume that this unknown scattering surface lies between the lines $\Gamma_0 := \{x_2 = 0\}$ and Γ_h for some $h > 0$. Let $\mathcal{I}_1(\alpha)$ and $\mathcal{I}_2(\alpha)$ be two admissible sets of elastic waves that are α-quasi-periodic. Given a fixed incident angle $\theta \in (-\pi/2, \pi/2)$, this paper is devoted to studying the following inverse problems $(\mathbf{P}_j)$ and $(\mathbf{S}_j)$, $j = 1, 2, 3$, by using $k_p \sin\theta$-quasi-periodic and $k_s \sin\theta$-quasi-periodic elastic waves.

($\mathbf{P}_1$) Determine Λ from the Rayleigh coefficients $A_{p,n}$, $n \in \mathbb{Z}$, of the compressional part of the scattered near-field on Γ_h corresponding to each incident elastic wave from the set $\mathcal{I}_1(\alpha)$ with $\alpha = k_p \sin\theta$.

($\mathbf{P}_2$) Determine Λ from the Rayleigh coefficients $A_{s,n}$, $n \in \mathbb{Z}$, of the shear part of the scattered near-field on Γ_h corresponding to each incident elastic wave from the set $\mathcal{I}_2(\alpha)$ with $\alpha = k_p \sin\theta$.

($\mathbf{P}_3$) Determine Λ from the Rayleigh coefficients $A_{p,n}, A_{s,n}$, $n \in \mathbb{Z}$, of the scattered near-field on Γ_h corresponding to each incident elastic wave from the set $\mathcal{I}_1(\alpha) \cup \mathcal{I}_2(\alpha)$ with $\alpha = k_p \sin\theta$.

The inverse problems $(\mathbf{S}_j)$ are formulated similarly as $(\mathbf{P}_j)$ with the quasi-periodicity parameter replaced by $\alpha = k_s \sin\theta$. Obviously, the scattering surface will be recovered by selecting appropriate incident waves depending on the source of the measurement data, that is, the component of the elastic waves providing us the information of the near-field data on Γ_h. Our aim is to establish the factorization method for $(\mathbf{P}_j)$ and $(\mathbf{S}_j)$ and compare the numerical results by using quasi-periodic incident waves with different phase-shifts and by using different components of the scattered field. The admissible sets $\mathcal{I}_j(\alpha)$ of incident waves will be explicitly defined in the next section.

3 The admissible sets of incident elastic waves

In contrast to the inverse scattering from bounded obstacles, the angle of incidence has to be restricted to $(-\pi/2, \pi/2)$ in order to identify the scattering surface from above. However, it seems not suitable to employ incident waves with distinct angles ranging from $(-\pi/2, \pi/2)$, since the quasi-periodicity of the scattered field varies with the angle of incidence. In the acoustic case, [5]) suggests using the following set of incident waves having a common phase shift

$$\left\{ u_n^{\mathrm{in}}(y) := \frac{i}{4\pi\beta_n}\left[e^{i(\alpha_n y_1 - \beta_n y_2)} - e^{i(\alpha_n y_1 + \beta_n y_2)}\right], \ \ n \in \mathbb{Z} \right\} \tag{9}$$

where β_n is defined as in (6) with k_p replaced by k. In (9), it is assumed that $\beta_n \neq 0$ for all $n \in \mathbb{Z}$, that is, the Rayleigh frequencies are excluded. Consequently, the periodic analogue version of the factorization method can be justified by using the single-layer potential whose kernel is the α-quasi-periodic Green's function to the Helmholtz equation $(\Delta + k^2)u = 0$ in a half-plane. Note that each function u_n^{in} in (9) satisfies the Dirichlet boundary condition on Γ_0 and consists of both upward and downward waves modes, using only the downward modes cannot lead to a desired factorization of the near-field operator to which an appropriate range identity can be applied. Recall the following α-quasi-periodic Green's function to the Helmholtz equation $\Delta u + k^2 u = 0$ (see e.g. [27])

$$G_k(x,y) = \frac{i}{4\pi}\sum_{n\in\mathbb{Z}} \frac{1}{\beta_n}\exp(i\alpha_n(x_1 - y_1) + i\beta_n|x_2 - y_2|), \quad x - y \neq n(2\pi, 0)^T$$

Then, the difference $G_k(x,y) - G_k(x,y')$, with $(y_1,y_2)' = (y_1,-y_2)$, is just the α-quasi-periodic Green's function in the half space $x_2 > 0$ satisfying the Dirichlet boundary condition on the boundary $x_2 = 0$. Observe further that, the incident wave $u_n^{in}(y)$ coincides with the conjugate of the n-th Rayleigh coefficient of the function $x \to G_k(x,y) - G(x,y')$ for $x_2 > y_2$. Inspired by these facts in acoustics, we introduce the following two admissible sets of incident elastic waves for (**P**$_j$) and (**S**$_j$), $j = 1,2,3$:

$$\mathcal{I}_j(\alpha) := \{u_{j,n}^{in}(y), \ n \in \mathbb{Z}\}, \quad j = 1,2$$

where $u_{1,n}^{in}(y)$ (or $u_{2,n}^{in}(y)$) is defined as the conjugate of the n-th Rayleigh coefficient of the compressional (or shear) part of the function $x \to \Pi_D(x,y)$ (or multiplied by some constant) for $x_2 > y_2 > 0$. Here, $\Pi_D(x,y)$ stands for the α-quasi-periodic half-space Green's tensor to the Navier equation with the Dirichlet boundary condition on Γ_0. The expression of $\Pi_D(x,y)$, which seems unknown by far in the literature, will be derived from the free-space elastic Green's tensor in the remaining part of this section.

We first recall the free space fundamental solution to the Navier equation (2) (see e.g., [4]),

$$\Gamma(x,y) = \frac{1}{\mu}\Phi_{k_s}(x,y)\, I + \frac{1}{\omega^2}\mathrm{grad}_x\mathrm{grad}_x^T\left[\Phi_{k_s}(x,y) - \Phi_{k_p}(x,y)\right]$$

where I, Φ_k stand for the 2×2 unit matrix and the free space fundamental solution to the Helmholtz equation, respectively. Then, the α-quasi-periodic fundamental solution (Green's tensor) to the Navier equation takes the form

$$\Pi(x,y) := \sum_{n\in\mathbb{Z}} \exp(-i\alpha 2\pi n)\,\Gamma(x + n(2\pi,0), y), \quad x - y \neq n(2\pi,0), \ \ n \in \mathbb{Z}.$$

See [3, Section 6] for the convergence analysis of the above series. Similarly to the form of $\Gamma(x, y)$, the tensor $\Pi(x, y)$ can be written as (see [12])

$$\begin{aligned}\Pi(x,y) &= \frac{1}{\mu}G_{k_s}(x,y)\,I + \frac{1}{\omega^2}\mathrm{grad}_x\mathrm{grad}_x^T\left[G_{k_s}(x,y) - G_{k_p}(x,y)\right] \\ &= \frac{1}{\mu}\begin{pmatrix} G_{k_s}(x,y) & 0 \\ 0 & G_{k_s}(x,y)\end{pmatrix} + \frac{1}{\omega^2}\begin{pmatrix} \partial_{x_1}^2 & \partial_{x_1}\partial_{x_2} \\ \partial_{x_2}\partial_{x_1} & \partial_{x_2}^2\end{pmatrix}\left[G_{k_s}(x,y) - G_{k_p}(x,y)\right]. \end{aligned} \tag{10}$$

To split the function $x \to \Pi(x, y)$ into its compressional and shear parts, we rewrite $\Pi(x, y)$ as

$$\begin{aligned}\Pi(x,y) = &\sum_{n\in\mathbb{Z}}\left\{(\alpha_n,\beta_n)^T\,P^{(n)}(y)\,W_{p,n}\,\exp(i(\alpha_n x_1 + \beta_n x_2))\right\} \\ &+\sum_{n\in\mathbb{Z}}\left\{(-\gamma_n,\alpha_n)^T\,S^{(n)}(y)\,W_{s,n}\,\exp(i(\alpha_n x_1 + \gamma_n x_2))\right\}\end{aligned} \tag{11}$$

for $x_2 > y_2$, where $P^n(y), S^n(y) \in \mathbb{C}^{1\times 2}$ will be referred to as the Rayleigh coefficients of the compressional and shear parts of $\Pi(x, y)$, respectively. Inserting the representation of $G_k(x, y)$ to (10), we find

$$\begin{aligned} P^n(y) = &\ \frac{i}{4\pi\omega^2\,W_{p,n}\,\beta_n}\,(\alpha_n,\beta_n)\,\exp(-i\alpha_n y_1 - i\beta_n y_2), \\ S^n(y) = &\ \frac{i}{4\pi\omega^2\,W_{s,n}\,\gamma_n}\,(-\gamma_n,\alpha_n)\,\exp(-i\alpha_n y_1 - i\gamma_n y_2)\end{aligned} \tag{12}$$

for $x_2 > y_2$. It is worthy pointing out that the difference $\Pi(x, y) - \Pi(x, y')$ is not the half-space Green's tensor to the Navier equation since it does not vanish on Γ_0 by virtue of the derivative with respect to x_2 acting on G_{k_s} and G_{k_p}. In [4], making use of the Fourier transform, Arens has derived the non-quasi-periodic half-plane Green's tensor of the form

$$\Gamma_D(x,y) = \Gamma(x,y) - \Gamma(x,y') + U(x,y), \quad x \neq y,\ x_2, y_2 > 0 \tag{13}$$

where the correction term $U(x, y)$ is defined as the integral

$$U(x,y) := -\frac{i}{2\pi\omega^2}\int_{-\infty}^{\infty}\Big(M_p(t,\eta_p(t),\,\eta_s(t);\,x_2,y_2) + M_s(t,\eta_p(t),\,\eta_s(t);\,x_2,y_2)\Big)\,e^{-i(x_1-y_1)t}\,\mathrm{d}t,$$

$$M_p(t,\eta_p(t),\,\eta_s(t);\,x_2,y_2) := \frac{e^{i\eta_p(t)\,(x_2+y_2)} - e^{i(\eta_p(t)\,x_2+\eta_s(t)\,y_2)}}{\eta_p(t)\,\eta_s(t)\,+t^2}\begin{pmatrix} -t^2\eta_s(t) & t^3 \\ t\eta_p(t)\,\eta_s(t) & -t^2\eta_p(t)\end{pmatrix},$$

$$M_s(t,\eta_p(t),\,\eta_s(t);\,x_2,y_2) := \frac{e^{i\eta_s(t)\,(x_2+y_2)} - e^{i(\eta_s(t)\,x_2+\eta_p(t)\,y_2)}}{\eta_p(t)\,\eta_s(t)\,+t^2}\begin{pmatrix} -t^2\eta_s(t) & -t\eta_p(t)\,\eta_s(t) \\ -t^3 & -t^2\eta_p(t)\end{pmatrix}$$

with

$$\eta_p(t) := \begin{cases}\sqrt{k_p^2 - t^2}, & t^2 \le k_p^2, \\ i\sqrt{t^2 - k_p^2}, & t^2 > k_p^2,\end{cases} \qquad \eta_s(t) := \begin{cases}\sqrt{k_s^2 - t^2}, & t^2 \le k_s^2 \\ i\sqrt{t^2 - k_s^2}, & t^2 > k_s^2\end{cases}$$

Motivated by this, we define the half-space α-quasi-periodic Green's tensor in the following way

$$\Pi_D(x,y) := \sum_{n\in\mathbb{Z}}\exp(-i\alpha 2\pi n)\,\Gamma_D(x + n(2\pi,0),y) = \Pi(x,y) - \Pi(x,y') + U_\alpha(x,y)$$

for $x-y\neq n(2\pi,0),\ n\in\mathbb{Z}$, where

$$U_\alpha(x,y):=\sum_{n\in\mathbb{Z}}\exp(-i\alpha 2\pi n)\,U(x+n(2\pi,0),y) \tag{14}$$

From Poisson's summation formula, we see

$$\sum_{n\in\mathbb{Z}}[\exp(-i\alpha 2\pi n)\exp(-i(x_1+2n\pi-y_1)t)]=\exp(-i(x_1-y_1)t)\sum_{n\in\mathbb{Z}}\delta(t+\alpha_n)$$

where $\delta(\cdot)$ denotes the Dirac delta function. Inserting the previous identity back to (14) yields an alternative expression of U_α:

$$\begin{aligned}U_\alpha(x,y)\quad:=\quad&\frac{i}{2\pi\omega^2}\sum_{n\in\mathbb{Z}}\left\{\left[e^{i(\alpha_n x_1+\beta_n x_2)}\big(e^{-i(\alpha_n y_1-\beta_n y_2)}-e^{-i(\alpha_n y_1-\gamma_n y_2)}\big)\begin{pmatrix}\alpha_n\gamma_n & \alpha_n^2\\ \beta_n\gamma_n & \alpha_n\beta_n\end{pmatrix}\right.\right.\\&\left.\left.+e^{i(\alpha_n x_1+\gamma_n x_2)}\big(e^{-i(\alpha_n y_1-\gamma_n y_2)}-e^{-i(\alpha_n y_1-\beta_n y_2)}\big)\begin{pmatrix}\alpha_n\gamma_n & -\gamma_n\beta_n\\ -\alpha_n^2 & \alpha_n\beta_n\end{pmatrix}\right]\frac{\alpha_n}{\alpha_n^2+\beta_n\gamma_n}\right\}\end{aligned}$$

for $x_2>y_2$. Hence, the n-th Rayleigh coefficients of the compressional and shear parts of the function $x\to U_\alpha(x,y)$ can be formulated as (cf. (7)):

$$\begin{aligned}\tilde{P}^{(n)}(y)\quad&=\quad\frac{i\,\alpha_n}{2\pi\omega^2}\,\frac{e^{-i(\alpha_n y_1-\beta_n y_2)}-e^{-i(\alpha_n y_1-\gamma_n y_2)}}{W_{p,n}\,(\alpha_n^2+\beta_n\gamma_n)}\,(\gamma_n,\alpha_n)^T,\\ \tilde{S}^{(n)}(y)\quad&=\quad-\frac{i\,\alpha_n}{2\pi\omega^2}\,\frac{e^{-i(\alpha_n y_1-\beta_n y_2)}-e^{-i(\alpha_n y_1-\gamma_n y_2)}}{W_{s,n}\,(\alpha_n^2+\beta_n\gamma_n)}\,(-\alpha_n,\beta_n)^T\end{aligned}$$

for $x_2>y_2$ with $W_{p,n},W_{s,n}$ given by (5).

To introduce our admissible sets of incident waves, as mentioned at the beginning of this section, we define $u^{in}_{1,n}(y)$ and $u^{in}_{2,n}(y)$ as the conjugate of the n-th Rayleigh coefficient of the compressional and shear part of the function $x\to\Pi_D(x,y)$, respectively. That is, after changing variables,

$$u^{in}_{1,n}(x):=\overline{P^{(n)}(x)-P^{(n)}(x')+\tilde{P}^{(n)}(x)},\quad u^{in}_{2,n}(x):=\overline{S^{(n)}(x)-S^{(n)}(x')+\tilde{S}^{(n)}(x)} \tag{15}$$

for $n\in\mathbb{Z}$, where $P^{(n)}$ and $S^{(n)}$ are defined as in (12). More precisely, we can write $u^{in}_{1,n}$ and $u^{in}_{2,n}$ as

$$\begin{aligned}u^{in}_{1,n}(x)=\quad&\frac{-i}{4\pi\omega^2\overline{\beta}_n\,\overline{W}_{p,n}}\big(u^{in}_{1,n,\mathsf{d}}(x)+u^{in}_{1,n,\mathsf{u}}(x)\big),\\ u^{in}_{2,n}(x)=\quad&\frac{-i}{4\pi\omega^2\overline{\gamma}_n\,\overline{W}_{s,n}}\big(u^{in}_{2,n,\mathsf{d}}(x)+u^{in}_{2,n,\mathsf{u}}(x)\big)\end{aligned} \tag{16}$$

with $u^{in}_{j,n,\mathsf{d}}$ and $u^{in}_{j,n,\mathsf{u}},\ j=1,2,n\in\mathbb{Z}$, denoting the downward and upward propagating modes, respectively, given by

$$u^{in}_{1,n,\mathsf{d}}(x)=\begin{cases}\frac{\alpha_n^2-\beta_n\gamma_n}{\alpha_n^2+\beta_n\gamma_n}\begin{pmatrix}-\alpha_n\\ \beta_n\end{pmatrix}e^{i(\alpha_n x_1-\beta_n x_2)}-\frac{2\alpha_n\beta_n}{\alpha_n^2+\beta_n\gamma_n}\begin{pmatrix}\gamma_n\\ \alpha_n\end{pmatrix}e^{i(\alpha_n x_1-\gamma_n x_2)}, & |\alpha_n|\le k_p,\\ \begin{pmatrix}\alpha_n\\ -\beta_n\end{pmatrix}e^{i(\alpha_n x_1-\beta_n x_2)}+\frac{2\alpha_n\beta_n}{\alpha_n^2-\beta_n\gamma_n}\begin{pmatrix}\gamma_n\\ \alpha_n\end{pmatrix}e^{i(\alpha_n x_1-\gamma_n x_2)}, & k_p<|\alpha_n|<k_s,\\ \begin{pmatrix}\alpha_n\\ -\beta_n\end{pmatrix}e^{i(\alpha_n x_1-\beta_n x_2)}, & |\alpha_n|\ge k_s\end{cases}$$

$$u^{in}_{1,n,\mathsf{u}}(x)=\begin{cases}\begin{pmatrix}\alpha_n\\ \beta_n\end{pmatrix}e^{i(\alpha_n x_1+\beta_n x_2)}, & |\alpha_n|\le k_p,\\ -\frac{\alpha_n^2+\beta_n\gamma_n}{\alpha_n^2-\beta_n\gamma_n}\begin{pmatrix}\alpha_n\\ \beta_n\end{pmatrix}e^{i(\alpha_n x_1+\beta_n x_2)}, & k_p<|\alpha_n|<k_s,\\ -\frac{\alpha_n^2-\beta_n\gamma_n}{\alpha_n^2+\beta_n\gamma_n}\begin{pmatrix}\alpha_n\\ \beta_n\end{pmatrix}e^{i(\alpha_n x_1+\beta_n x_2)}-\frac{2\alpha_n\beta_n}{\alpha_n^2+\beta_n\gamma_n}\begin{pmatrix}\gamma_n\\ -\alpha_n\end{pmatrix}e^{i(\alpha_n x_1+\gamma_n x_2)}, & |\alpha_n|\ge k_s\end{cases}$$

and

$$u^{in}_{2,n,\mathsf{d}}(x)=\begin{cases}\frac{\alpha_n^2-\beta_n\gamma_n}{\alpha_n^2+\beta_n\gamma_n}\begin{pmatrix}\gamma_n\\ \alpha_n\end{pmatrix}e^{i(\alpha_n x_1-\gamma_n x_2)}-\frac{2\alpha_n\gamma_n}{\alpha_n^2+\beta_n\gamma_n}\begin{pmatrix}\alpha_n\\ -\beta_n\end{pmatrix}e^{i(\alpha_n x_1-\beta_n x_2)}, & |\alpha_n|\le k_p,\\ \frac{\alpha_n^2+\beta_n\gamma_n}{\alpha_n^2-\beta_n\gamma_n}\begin{pmatrix}\gamma_n\\ \alpha_n\end{pmatrix}e^{i(\alpha_n x_1-\gamma_n x_2)}, & k_p<|\alpha_n|<k_s,\\ -\begin{pmatrix}\gamma_n\\ \alpha_n\end{pmatrix}e^{i(\alpha_n x_1-\gamma_n x_2)}, & |\alpha_n|\ge k_s\end{cases}$$

$$u^{in}_{2,n,\mathsf{u}}(x)=\begin{cases}\begin{pmatrix}\gamma_n\\ -\alpha_n\end{pmatrix}e^{i(\alpha_n x_1+\gamma_n x_2)}, & |\alpha_n|\le k_p,\\ \begin{pmatrix}\gamma_n\\ -\alpha_n\end{pmatrix}e^{i(\alpha_n x_1+\gamma_n x_2)}-\frac{2\alpha_n\gamma_n}{\alpha_n^2-\beta_n\gamma_n}\begin{pmatrix}\alpha_n\\ \beta_n\end{pmatrix}e^{i(\alpha_n x_1+\beta_n x_2)}, & k_p<|\alpha_n|<k_s,\\ \frac{\alpha_n^2-\beta_n\gamma_n}{\alpha_n^2+\beta_n\gamma_n}\begin{pmatrix}-\gamma_n\\ \alpha_n\end{pmatrix}e^{i(\alpha_n x_1+\gamma_n x_2)}+\frac{2\alpha_n\gamma_n}{\alpha_n^2+\beta_n\gamma_n}\begin{pmatrix}\alpha_n\\ \beta_n\end{pmatrix}e^{i(\alpha_n x_1+\beta_n x_2)}, & |\alpha_n|\ge k_s.\end{cases}$$

It can be readily checked that $u^{in}_{j,n}$ are α-quasi-periodic solutions to the Navier equation with the Dirichlet boundary condition on Γ_0. Note that, for the inverse problems (**P**$_j$) and (**S**$_j$), $j=1,2$, both compressional and shear waves are involved in the incident elastic wave $u^{in}_{j,n}$, $n\in\mathbb{Z}$ although the measurement data only come from the compressional part when $j=1$ or the shear part in the case $j=2$.

Since the upward modes occurring in $u^{in}_{j,n}$ ($j=1,2$) are not physically meaningful incoming waves from Ω_Λ, the scattered field $u^{sc}_{j,n}$ due to $u^{in}_{j,n}$ cannot be generated straightforwardly. Denoting by $\widetilde{u}^{sc}_{j,n}$ the scattered field corresponding to $u^{in}_{j,n,\mathsf{d}}$, we have

$$u^{sc}_{1,n}=\frac{-i}{4\pi\omega^2\overline{\beta}_n\,\overline{W}_{p,n}}(\widetilde{u}^{sc}_{1,n}-u^{in}_{1,n,\mathsf{u}}),\ u^{sc}_{s,n}=\frac{-i}{4\pi\omega^2\overline{\gamma}_n\,\overline{W}_{s,n}}(\widetilde{u}^{sc}_{2,n}-u^{in}_{2,n,\mathsf{u}}),\ n\in\mathbb{Z}$$

due to the linearity of the scattering solution with respect to incident waves. As a consequence, the m-th Rayleigh coefficients $A^{j,n}_{p,m}$, $A^{j,n}_{s,m}$ of $u^{sc}_{j,n}$ can be written as

$$A^{j,n}_{p,m}=\frac{-i}{4\pi\omega^2\overline{\beta}_n\,W_{p,n}}(\widetilde{A}^{j,n}_{p,m}-\widehat{A}^{p,n}_{p,m}),\quad A^{j,n}_{s,m}=\frac{-i}{4\pi\omega^2\overline{\gamma}_n\,W_{s,n}}(\widetilde{A}^{j,n}_{s,m}-\widehat{A}^{p,n}_{s,m})$$

for $m,n\in\mathbb{Z}$, $j=1,2$, where $\widetilde{A}^{j,n}_{p,m}$ and $\widehat{A}^{j,n}_{p,m}$ (resp. $\widetilde{A}^{j,n}_{s,m}$ and $\widehat{A}^{j,n}_{s,m}$) denote the m-th Rayleigh coefficients of the compressional (resp. shear) part of $\tilde{u}^{sc}_{j,n}$ and $u^{in}_{j,n,\mathsf{u}}$, respectively.

We end up this section by introducing several single-layer potentials. With the Green's tensor Π, we define the periodic single-layer potential

$$(\mathsf{SL}\varphi)(x):=\int_\Lambda \Pi(x,y)\varphi(y)ds(y),\quad x\in\Omega_\Lambda \tag{17}$$

and the corresponding single-layer operator $\mathcal{S}\varphi(x)=\mathsf{SL}\varphi(x)|_\Lambda$. Similarly, one can define integral operators SL_D and $\mathcal{S}_D$ with the kernel Π replaced by the half-space Green's tensor Π_D. In what follows, we sometimes employ the notation $\mathsf{SL}^{(\omega)}$, $\mathsf{SL}^{(\omega)}_D$, $\mathcal{S}^{(\omega)}$ and $\mathcal{S}^{(\omega)}_D$ to indicate their dependence on the frequency ω.

4 The factorization method

Since the inverse problems (**P**$_j$) and (**S**$_j$) ($j = 1, 2, 3$) are quite similar, we will only investigate the factorization method for the inverse problems (**P**$_j$). With necessary changes on the quasi-periodicity the mathematical argument automatically carries over to the second class problems (**S**$_j$). Hence, unless otherwise stated we always assume $\alpha = k_p \sin\theta$ for some fixed $\theta \in (-\pi/2, \pi/2)$. The unknown scattering surface will be retrieved from the information of the Rayleigh coefficients of the scattered P- or S-waves due to each incident elastic wave from the admissible set $\mathcal{I}_1(\alpha)$ or $\mathcal{I}_2(\alpha)$ of α-quasi-periodic functions proposed in Section 3.

Thanks to the periodicity of the grating profile and the α-quasi-periodicity of the solutions, our discussions can be restricted to one periodic cell. Consequently, we redefine the region and the boundary as

$$\Omega := \{x \in \mathbb{R}^2 : x_1 \in (0, 2\pi), x_2 > f(x_1) > 0\}, \quad \Lambda := \{x \in \mathbb{R}^2 : x_1 \in (0, 2\pi), x_2 = f(x_1)\}$$

Introduce the finite line $\Gamma_h := \{x \in \mathbb{R}^2 : x_1 \in (0, 2\pi), x_2 = h\}$ for some $h > \Lambda^+$ on which the near-field data are measured, and set $\Omega_h := \Omega_h^+ \cup \Lambda \cup \Omega_{-h}^-$, where

$$\Omega_h^+ := \{x \in \mathbb{R}^2 : x_1 \in (0, 2\pi),\ 0 < f(x_1) < x_2 < h\},$$
$$\Omega_{-h}^- := \{x \in \mathbb{R}^2 : x_1 \in (0, 2\pi),\ -h < x_2 < f(x_1)\}$$

For $s \in \mathbb{R}$, let $H_\alpha^s(\cdot)$ denote the Sobolev spaces of scalar functions on the domain $(\cdot)$ which are α-quasi-periodic with respect to x_1. Analogously to the factorization method for bounded obstacle scattering problems, we define the periodic version of the so-called data-to-pattern operator G_j, the Herglotz operator H_j and the near-field operator N_j for (**P**$_j$), $j = 1, 2, 3$.

Definition 4.1. *The data-to-pattern operators $G_j : H_\alpha^{1/2}(\Lambda)^2 \to l^2, j = 1, 2$, are defined as*

$$G_1(\varphi) = \{A_{p,n} : n \in \mathbb{Z}\}, \quad G_2(\varphi) = \{A_{s,n} : n \in \mathbb{Z}\}, \quad \varphi \in H_\alpha^{1/2}(\Lambda)^2$$

where $A_{p,n}$ and $A_{s,n}$ denote the n-th Rayleigh coefficients of the compressional and shear part of the unique scattered field u^{sc} to the problem (2) with the boundary value data $u^{sc} = \varphi$ on Λ. The operator $G_3 : H_\alpha^{1/2}(\Lambda)^2 \to l^2 \times l^2$ is defined as the product of G_1 and G_2, that is, $G_3 := G_1 \times G_2$.

Definition 4.2. *With the incident waves $u_{j,n}^{in}$ given in* (16)*, the Herglotz operators $H_j : l^2 \to H_\alpha^{1/2}(\Lambda)^2$ for $j = 1, 2$ and $H_3 : l^2 \times l^2 \to H_\alpha^{1/2}(\Lambda)^2$ are defined as*

$$[H_j(\boldsymbol{b})](x) := \sum_{n \in \mathbb{Z}} b_n\, u_{j,n}^{in}(x), \quad j = 1, 2, \quad H_3(\boldsymbol{a}, \boldsymbol{b}) := H_1(\boldsymbol{a}) + H_2(\boldsymbol{b}), \quad x \in \Lambda$$

for $\boldsymbol{a} = (a_n)_{n\in\mathbb{Z}},\ \boldsymbol{b} = (b_n)_{n\in\mathbb{Z}} \in l^2$.

Definition 4.3. *Define the near-field operators $N_j : l^2 \to l^2, j = 1, 2$, and $N_3 : l^2 \times l^2 \to l^2 \times l^2$ as*

$$N_j = -G_j H_j, \quad j = 1, 2, 3$$

The Herglotz operator H_3 is a supposition of $k_p \sin\theta$-quasi-periodic incident waves $u_{1,n}^{in}$ and the $k_s \sin\theta$-quasi-periodic ones $u_{2,n}^{in}$ with different weights. The near field operator N_j ($j = 1, 2$) maps the supposition of the incident waves $u_{j,n}^{in}$ to the Rayleigh coefficients of the compressional part ($j = 1$) or shear part ($j = 2$) of the associated scattered field.

In view of the Green's tensor $\Pi(x,y)$ given in (11), we can explicitly formulate the Rayleigh coefficients $C_{p,n}(y), C_{s,n}(y)$ of the compressional and shear parts of the function $x \to \Pi(x,y)\mathbf{C}$, where $\mathbf{C} \in \mathbb{C}^{2\times 1}$, as

$$\begin{aligned} C_{p,n}(y) = & \quad \frac{i}{4\pi\omega^2\beta_n W_{p,n}} \exp(-iy\cdot(\alpha_n,\beta_n)^T)\,[(\alpha_n,\beta_n)^T\cdot\mathbf{C}], \\ C_{s,n}(y) = & \quad \frac{i}{4\pi\omega^2\gamma_n W_{s,n}} \exp(-iy\cdot(\alpha_n,\gamma_n)^T)\,[(-\gamma_n,\alpha_n)^T\cdot\mathbf{C}] \end{aligned} \tag{18}$$

for $x_2 > y_2 > 0$. The sequences $C_{p,n}$ and $C_{s,n}$ can be utilized to characterize the region beneath the scattering surface.

Lemma 4.4. *For any fixed non-zero complex vector* $\mathbf{C}$*, the sequence* $\{C_{p,n}(y)\}_{n\in\mathbb{Z}}$ *(resp.* $\{C_{s,n}(y)\}_{n\in\mathbb{Z}}$*) lies in the range of* G_1 *(resp.* G_2*) if and only if* $y \in \mathbb{R}^2\backslash\overline{\Omega}$*. Consequently, the sequence* $\{C_{p,n}(y)\}_{n\in\mathbb{Z}} \times \{C_{s,n}(y)\}_{n\in\mathbb{Z}}$ *lies in the range of* G_3 *if and only if* $y \in \mathbb{R}^2\backslash\overline{\Omega}$*.*

Proof. We only need to consider the sequence $\{C_{p,n}(y) : n \in \mathbb{Z}\}$ since the other cases can be dealt with similarly. Obviously, we have $\{C_{p,n}(y) : n \in \mathbb{Z}\} \in l^2$ whenever $y_2 < h$. If $y \in \mathbb{R}^2\backslash\overline{\Omega}$, then $\{C_{p,n}(y) : n \in \mathbb{Z}\} = N_1(\varphi)$ with $\varphi = (\Pi(x,y)\mathbf{C})|_\Lambda \in H_\alpha^{1/2}(\Lambda)^2$.

Assume that $\{C_{p,n}(y) : n \in \mathbb{Z}\} = N_1(\tilde{\varphi})$ for some $\tilde{\varphi} \in H_\alpha^{1/2}(\Lambda)^2$ and $y \in \overline{\Omega_h^+}$. Denote by $\Pi_P^C(x)$ the pressure part of the function $\Pi(x,y)\mathbf{C}$ restricted to Γ_h and by u^{sc} the scattered field to the problem (2) with the boundary data $u^{sc} = \tilde{\varphi}$ on Λ. The coincidence of $\Pi_P^C(x)$ with the compressional part u_p^{sc} of u^{sc} on Γ_h implies that $\Pi_P^C(x) = u_p^{sc}$ in $x_2 > h$, due to the uniqueness of the Dirichlet boundary value problem in a half plane. Together with the unique continuation of solutions to the Helmholtz equation, this further yields the fact that $\Pi_P^C(x) = u_p^{sc}$ in $\Omega_h^+\backslash\{y\}$. On one hand, we have $\operatorname{div} u_p^{sc} = \operatorname{div} u^{sc} \in L^2_{loc}(\Omega_h^+)$. On the other hand, $\operatorname{div} \Pi_P^C(x) = \operatorname{div}_x[\Pi(x,y)\mathbf{C}] \notin L^2_{loc}(\Omega_h^+)$ since the shear part of u^{sc} is divergence-free and $\operatorname{div}_x[\Pi(x,y)\mathbf{C}] \sim \mathcal{O}(|x-y|^{-1})$ as $x \to y$ in $\Omega_h^+\backslash\{y\}$. This contradiction gives that $y \in \mathbb{R}^2\backslash\overline{\Omega}$. □

By Lemma 4.4, the periodic profile Λ can be identified theoretically from the range of G_j, which, however, cannot be numerically implemented. The essence of the factorization method is to connect the range of N_j with that of G_j so that the scattering surface can be retrieved from the spectral of N_j. To that end, we will factorize N_j in terms of G_j as shown in the following lemma, and then apply proper range identities. In the following, H_j^* ($j = 1,2,3$) denotes the adjoint operator of H_j, and the single-layer operator $\mathcal{S}_D$ is defined at the end of Section 3.

Lemma 4.5. *It holds that* $H_j^* = G_j\mathcal{S}_D$ *and the factorization* $N_j = -G_j\mathcal{S}_D^*G_j^*$ *for* $j = 1,2,3$*.*

Proof. For $\varphi \in H_\alpha^{-1/2}(\Lambda)^2$, let $(G_j\mathcal{S}_D\varphi)_n$ represent the n-th Rayleigh coefficient of $G_j\mathcal{S}_D(\varphi)$, $j = 1,2$. From the definitions of $\mathcal{S}_D$, G_j and $u_{j,n}^{in}$ we deduce that (cf. (15))

$$(G_j\mathcal{S}_D\varphi)_n = \int_\Lambda \overline{u_{j,n}^{in}}\cdot\varphi\,ds, \quad j = 1,2$$

The relations $H_j^* = G_j\mathcal{S}_D$, $j = 1,2$, then follow directly from the previous identity and the definition of H_j, which further yield the factorizations $N_j = -G_jH_j = -G_j\mathcal{S}_D^*G_j^*$. From the definitions of H_3 and G_3, we arrive at the result that $H_3^* = H_1^* \times H_2^* = G_3\mathcal{S}_D$ and thus $N_3 = -G_3H_3 = -G_3\mathcal{S}_D^*G_3^*$. □

We now introduce the concept of the Dirichlet eigenvalue for quasi-periodic Lam$\acute{e}$ operators over a periodic domain.

Definition 4.6. *The frequency of incidence ω is called a Dirichlet eigenvalue of the α-quasi-periodic Lam$\acute{e}$ operator over the periodic layer $\Omega_0^- := \{x : 0 < x_2 < f(x_1), 0 < x_1 < 2\pi\}$, if there exists a non-trivial α-quasi-periodic solution u to the Navier equation (2) on Ω_0^- such that $u = 0$ on Λ and Γ_0. Accordingly, u is called the Dirichlet eigenfunction with phase-shift α.*

Using variational arguments and standard spectral theory for compact operators, one can show that the Dirichlet eigenvalues form a countable set and the positive eigenvalues can be represented in terms of a min-max principle (see [10]). A further investigation of the monotonicity of these eigenvalues in [10] leads to Schiffer's uniqueness theorem for the inverse elastic scattering by rigid periodic surfaces. For the inverse problems (**P**$_j$), we make the following assumption:

Assumption (A): The frequency ω is not the Dirichlet eigenvalue of the quasi-periodic Lam$\acute{e}$ operator over the periodic region Ω_0^- with phase-shift $\alpha = k_p \sin\theta$.

This assumption will be used to verify the injectivity of the single-layer operator $\mathcal{S}_D$; see Lemma (4.7) (iii) and Remark 4.8 below. Before describing properties of the middle operator $\mathcal{S}_D^*$ involved in the factorization $N_j = -G_j \mathcal{S}_D^* G_j^*$, we recall that the real and imaginary parts of an operator T on a Hilbert space are defied as

$$\mathrm{Re}\,(T) := (T + T^*)/2, \quad \mathrm{Im}\,(T) := (T - T^*)/(2i)$$

Let the dual form $\langle \cdot, \cdot \rangle$ denote the dual pair between $H_\alpha^{-1/2}(\Lambda)^2$ and $H_\alpha^{1/2}(\Lambda)^2$ which extends the inner product of $L^2(\Lambda)^2$.

Lemma 4.7. *(i) There exist an angle $\phi \in (0, \pi/2)$ and a sufficiently small frequency $\omega_0 > 0$ such that the real part of the operator $\exp(-i\phi)\mathcal{S}^{(\omega)}$ is self-adjoint and positive definite when $\omega \in (0, \omega_0]$. Particularly, there exists a constant $c > 0$ such that*

$$\mathrm{Re}\,\langle \varphi, \exp(-i\phi)\mathcal{S}^{(\omega)}\varphi \rangle \geq c\,\omega\, \|\varphi\|^2_{H_\alpha^{-1/2}(\Lambda)^2} \quad \forall\, \varphi \in H_\alpha^{-1/2}(\Lambda)^2,\, \forall\, \omega \in (0, \omega_0] \tag{19}$$

(ii) For any $\omega' \in (0, \omega_0]$, the operator ${\mathcal{S}_\mathcal{D}}^{(\omega)} - \mathcal{S}^{(\omega')}$ is compact from $H_\alpha^{-1/2}(\Lambda)^2$ to $H_\alpha^{1/2}(\Lambda)^2$, and thus $\mathcal{S}_D$ is a Fredholm operator with index zero.

(iii) Under the assumption (A), the middle operator $-\mathcal{S}_D^* : H_\alpha^{-1/2}(\Lambda)^2 \to H_\alpha^{1/2}(\Lambda)^2$ is injective.

(iv) $-\mathrm{Im}\,(\mathcal{S}_D^*)$ is non-negative over $H_\alpha^{-1/2}(\Lambda)^2$, that is,

$$-\langle \varphi, \mathrm{Im}\,({\mathcal{S}_\mathcal{D}}^*)\varphi \rangle \geq 0 \quad \textit{for all} \quad \varphi \in H_\alpha^{-1/2}(\Lambda)^2$$

Proof. (i) Define $u(x) := \mathsf{SL}^{(\omega)}\varphi(x),\ x \in \mathbb{R}^2$. Then u satisfies the Navier equation in $\mathbb{R}^2\backslash\Lambda$, the upward Rayleigh expansion (4) for $x_2 > \Lambda^+$ and an analogous downward Rayleigh expansion in $x_2 < \Lambda^- := \min_{x\in\Lambda}\{x_2\}$. From the first Betti's formula and the jump relations for periodic single-layer potentials, it follows that

$$\begin{aligned}\langle \varphi, \mathcal{S}^{(\omega)}\varphi \rangle &= \int_\Lambda (\partial_\nu u^+ - \partial_\nu u^-) \cdot \overline{u}\, ds \\ &= \int_{\Omega_h} \left[\mathcal{E}(u, \overline{u}) - \omega^2 |u|^2\right]\, dx - \int_{\Gamma_h} \mathcal{T}_\omega^+ u \cdot \overline{u}\, ds - \int_{\Gamma_{-h}} \mathcal{T}_\omega^- u \cdot \overline{u}\, ds\end{aligned}$$

where $\mathcal{E}(\cdot,\cdot)$ is the bilinear form defined by

$$\begin{aligned}\mathcal{E}(u,v) &= (2\mu+\lambda)(\partial_1 u_1\partial_1\varphi_1+\partial_2 u_2\partial_2\varphi_2)+\mu(\partial_2 u_1\partial_2\varphi_1+\partial_1 u_2\partial_1\varphi_2)\\ &\quad +\mu(\partial_2 u_1\partial_1\varphi_2+\partial_1 u_2\partial_2\varphi_1)+\lambda(\partial_1 u_1\partial_2\varphi_2+\partial_2 u_2\partial_1\varphi_1)\end{aligned}$$

and $\mathcal{T}_\omega^\pm$ are the Dirichlet-to-Neumann maps defined on $\Gamma_{\pm h}$, respectively, and given by (see [12])

$$\mathcal{T}_\omega^\pm v = -\sum_{n\in\mathbb{Z}} M_{n,\omega}\widehat{v}_n \exp(i\alpha_n x_1) \quad \text{for} \quad v=\sum_{n\in\mathbb{Z}}\widehat{v}_n\exp(i\alpha_n x_1)\in H_\alpha^{1/2}(\Gamma_{\pm h})^2 \tag{20}$$

with the matrices $M_{n,\omega}\in\mathbb{C}^{2\times 2}$ of the form

$$M_{n,\omega} := \frac{1}{i}\begin{pmatrix} \omega^2\beta_n/t_n & 2\mu\alpha_n-\omega^2\alpha_n/t_n \\ -2\mu\alpha_n+\omega^2\alpha_n/t_n & \omega^2\gamma_n/t_n\end{pmatrix}, \quad t_n=\alpha_n^2+\beta_n\gamma_n \tag{21}$$

Consequently,

$$\begin{aligned}\mathrm{Re}\,\langle\varphi,\exp(-i\phi)\mathcal{S}^{(\omega)}\varphi\rangle &= \cos\phi\int_{\Omega_h}\left[\mathcal{E}(u,\overline{u})-\omega^2|u|^2\right]\,dx\\ &\quad -\mathrm{Re}\left\{\exp(i\phi)\int_{\Gamma_h\cup\Gamma_{-h}}\mathcal{T}_\omega^\pm u\cdot\overline{u}\,ds\right\}.\end{aligned} \tag{22}$$

We claim that there exist $\phi\in(0,\pi/2)$ and $\omega_*>0$ such that for all $u\in H_\alpha^{1/2}(\Gamma_{\pm h})^2$ and $\omega\in(0,\omega_*]$ there holds the inequality

$$-\mathrm{Re}\left\{\exp(i\phi)\int_{\Gamma_{\pm h}}\mathcal{T}_\omega^\pm u\cdot\overline{u}\,ds\right\}\geq c\,\omega\|u\|^2_{H_\alpha^{1/2}(\Gamma_{\pm h})^2} \tag{23}$$

with some constant $c>0$ independent of ω and u; see Lemma (A.1) (i) in the appendix for the proof. By the Friedrich-type inequality for the Navier equation (see, e.g. [12, Remark 2]), it follows from (22) and (23) that

$$\mathrm{Re}\,\langle\varphi,\exp(-i\phi)\mathcal{S}^{(\omega)}\varphi\rangle\geq\widetilde{c}\,\omega\,\|u\|^2_{H^1(\Omega_h)^2}-\omega^2\|u\|^2_{L^2(\Omega_h)^2},\quad \tilde{c}>0 \tag{24}$$

Now the estimate (19) follows from (24) for some sufficiently small positive number ω_0.

(ii) We write $\mathcal{S}_D^{(\omega)}-\mathcal{S}^{(\omega')}=\mathcal{S}_D^{(\omega)}-\mathcal{S}^{(\omega)}+\mathcal{S}^{(\omega)}-\mathcal{S}^{(\omega')}$. From the definitions of $\mathcal{S}_D^{(\omega)}$ and $\mathcal{S}^{(\omega)}$, we see that the kernels of $\mathcal{S}_D^{(\omega)}-\mathcal{S}^{(\omega)}$ and $\mathcal{S}^{(\omega)}-\mathcal{S}^{(\omega')}$ are both smooth. Hence, $\mathcal{S}_D^{(\omega)}-\mathcal{S}^{(\omega')}$ is compact from $H_\alpha^{-1/2}(\Lambda)^2$ to $H_\alpha^{1/2}(\Lambda)^2$, so by (i), $\mathcal{S}_D^{(\omega)}$ is a Fredholm operator with index of zero.

(iii) Since $\mathcal{S}_D$ is a Fredholm operator with index zero, we have $\dim(\mathrm{Ker}(\mathcal{S}_D))=\dim(\mathrm{Ker}(\mathcal{S}_D^*))$. Hence it suffices to prove the injectivity of $\mathcal{S}_D$. Define the single-layer potential $u(x)=\mathrm{SL}_D\varphi(x)$ for $x\in\mathbb{R}^2$. If $\mathcal{S}_D\varphi=0$ on Λ, then $u=0$ on Λ. Moreover, we have $u=0$ in Ω_h^+ due to the uniqueness of the forward scattering problem. Observing that u satisfies the Navier equation on Ω_0^- and vanishes on Λ and Λ_0, we get $u=0$ in Ω_0^- by Assumption (A). The jump relations for SL_φ finally yield $\varphi=0$ on Λ.

(iv) For $\varphi\in H_\alpha^{-1/2}(\Lambda)^2$, there holds

$$-\langle\varphi,\mathrm{Im}\,(\mathcal{S}_D^*)\varphi\rangle=\mathrm{Im}\,\langle\varphi,\mathcal{S}_D^*\varphi\rangle=\mathrm{Im}\,\langle\mathcal{S}_D\varphi,\varphi\rangle=-\mathrm{Im}\,\langle\varphi,\mathcal{S}_D\varphi\rangle.$$

Thus we only need to prove that $-\mathrm{Im}\,\langle\varphi,\mathcal{S}_D\varphi\rangle \geq 0$ To this end, define $u(x) := \mathsf{SL}_D^{(\omega)}\varphi(x),\ x\in\mathbb{R}^2$. Arguing similarly as in (i) with Γ_{-h} replaced by Γ_0 and using the fact that u vanishes on Γ_0, we obtain

$$-\mathrm{Im}\,\langle\varphi,\mathcal{S}_D\varphi\rangle = \mathrm{Im}\int_{\Gamma_h}\mathcal{T}u\cdot\overline{u}\,ds = 2\pi\omega^2\left(\sum_{|\alpha_n|<k_p}\beta_n|A_{p,n}|^2+\sum_{|\alpha_n|<k_s}\gamma_n|A_{s,n}|^2\right)\geq 0$$

where the last equality was proved in [12], and $A_{p,n},\ A_{s,n}$ denote the Rayleigh coefficients of the compressional and shear parts of u, respectively. □

Remark 4.8. To prove the injectivity of $\mathcal{S}_D$, we think it is necessary to make the assumption (**A**); see the proof of Lemma 4.7 (iii). Note that the single-layer potential (17) consists of both upward and downward modes in the region $-f(x_1) < x_2 < f(x_1)$ and is non-analytic not only on the curve $x_2 = f(x_1)$ but also on $x_2 = -f(x_1)$. An analogous assumption to Assumption (**A**) above could be used to close a gap in the proof of [5, Lemma 2.5 (i)], where a half-space quasi-periodic Green's function for the Helmholtz equation is involved.

Before stating the range identity, we need the following compactness and denseness results of the data-to-pattern operators G_j, that is,

Lemma 4.9. *The operators G_j for $j = 1,2,3$ are all compact and have a dense range.*

Lemma 4.9 can be proved in a standard way; see [28, Chapter 2] for a proof in the inverse acoustic scattering from penetrable diffraction gratings, which can be readily adapted to the Navier equation case. Lemmas 4.7 and 4.9 allow us to directly apply the range identity of [30, Theorem 3.4.1] to the factorization of the near-field operators N_j established in Lemma 4.5. The following abstract range identity generalizes the one contained in [28, Chapter 1], the proof of which is essentially based on the approach of Kirsch and Grinberg [26, Theorem 2.15] (cf. [30]).

Lemma 4.10 (**Range Identity**). *Let $X\subset U\subset X^*$ be a Gelfand triple with Hilbert space U and reflexive Banach space X such that the embedding is dense. Furthermore, let Y be a second Hilbert space and $F: Y\to Y$, $G: X\to Y$ and $T: X^*\to X$ be linear and bounded operators with $F = GTG^*$. Suppose further that*

(a) *G is compact and has a dense range.*

(b) *There exists $t\in(0,2\pi)$ with $\cos t\neq 0$ such that $\mathrm{Re}\,[\exp(it)T]$ has the form $\mathrm{Re}\,[\exp(it)T] = T_0+T_1$ with some compact operator T_1 and some coercive operator $T_0: X^*\to X$, that is there exists $c>0$ with*

$$\langle\varphi,T_0\varphi\rangle \geq c\|\varphi\|^2 \quad \textit{for all} \quad X^* \tag{25}$$

(c) *$\mathrm{Im}\,(T)$ is non-negative on X, that is, $\langle\mathrm{Im}\,(T)\varphi,\varphi\rangle\geq 0$ for all $\varphi\in X$. Moreover, we assume that one of the following conditions is fulfilled.*

(d) *T is injective.*

(e) *$\mathrm{Im}\,(T)$ is positive on the finite dimensional null space of $\mathrm{Re}\,[\exp(it)T]$, that is, for all $\varphi\neq 0$ such that $\mathrm{Re}\,[\exp(it)T]\varphi = 0$ we have $\langle\mathrm{Im}\,(T)\varphi,\varphi\rangle > 0$.*

Then the operator $F_\sharp := |\mathrm{Re}\,[\exp(it)F]| + \mathrm{Im}\,(F)$ is positive definite, and the ranges of $G : X \to Y$ and $F_\sharp^{1/2} : Y \to Y$ coincide.

Making use of Lemma 4.10, we can characterize the region beneath the periodic scattering surface in term of the spectrum of the near-field operators N_j, $j = 1, 2, 3$.

Theorem 4.11. *Let the assumption (**A**) hold and define the sequences $\{C_{p,n}(z)\}_{n\in\mathbb{Z}}$, $\{C_{s,n}(z)\}_{n\in\mathbb{Z}}$ as in* (18)*. Then the point $z \in \mathbb{R}^2\backslash\overline{\Omega}_\Lambda$ if and only if one of the following conditions holds:*

(i) $\{C_{p,n}(z)\}_{n\in\mathbb{Z}} \in \mathcal{R}[(N_{1\sharp})^{1/2}]$,

(ii) $\{C_{s,n}(z)\}_{n\in\mathbb{Z}} \in \mathcal{R}[(N_{2\sharp})^{1/2}]$,

(iii) $\{C_{p,n}(z)\}_{n\in\mathbb{Z}} \times \{C_{s,n}(z)\}_{n\in\mathbb{Z}} \in \mathcal{R}[(N_{3\sharp})^{1/2}]$.

where $N_{j\sharp} := |\mathrm{Re}\,[\exp(it)N_j]| + \mathrm{Im}\,(N_j)$, $j = 1, 2, 3,$ and $\mathcal{R}[\cdot]$ denotes the range of an operator.

Proof. By Lemma 4.4, it suffices to verify the coincidence of the ranges of $(N_{j\sharp})^{1/2}$ and G_j for $j = 1, 2, 3$. To do this, we shall apply Lemma 4.10 to the factorizations $N_j = -G_j\mathcal{S}_D^* G_j^*$ by verifying the conditions (a), (b), (c) and (d) with $T = -\mathcal{S}_D^*$, $F = N_j$ and $G = G_j$ for $j = 1, 2, 3$. The condition (a) follows from Lemma 4.9, while the conditions (c) and (d) follow from Lemma 4.7 (iv) and (iii), respectively. It remains to verify the condition (b). Indeed, letting $\omega_1 \in (0, \omega_0]$ and $\phi \in (0, \pi/2)$ be given as in Lemma 4.7, we get

$$-\mathrm{Re}\,\langle \varphi, \exp(it)\mathcal{S}^{(\omega_1)^*}\varphi\rangle = -\mathrm{Re}\,\langle \exp(-it)\mathcal{S}^{(\omega_1)}\varphi, \varphi\rangle = \mathrm{Re}\,\langle \varphi, \exp(-i(t-\pi))\mathcal{S}^{(\omega_1)}\varphi\rangle \qquad (26)$$

for all $\varphi \in H_\alpha^{-1/2}(\Lambda)^2$. Taking $t = \pi + \phi \in (\pi, 3/2\pi)$ in (26), we then conclude from (19) and the previous identity that

$$-\mathrm{Re}\,\langle \varphi, \exp(it)\mathcal{S}^{(\omega_1)^*}\varphi\rangle \geq c\,\|\varphi\|^2_{H_\alpha^{-1/2}(\Lambda)^2}, \quad c > 0$$

This, together with Lemma 4.7 (ii), implies the condition (b) in Lemma 4.10 with $T_0 = -\mathrm{Re}\,[\exp(it)\mathcal{S}^{(\omega_1)^*}]$. □

Let $(\sigma_n^{(j)}, \mathbf{e}_n^{(j)})$ be the eigensystem of $N_{j\sharp}$. By Picard's range criterion, the scattering surface Λ can be reconstructed by first selecting sampling points from the set $\{(z_1, z_2) \in \mathbb{R}^2 : 0 < z_2 < h\}$ and then computing one of the following indicator functions:

(i) $W_1(z) := \sum_{n=1}^\infty \left\{|\langle\{C_{p,n}(z)\}_{n\in\mathbb{Z}}, \{\mathbf{e}_n^{(1)}\}_{n\in\mathbb{Z}}\rangle_{l^2}|^2/\sigma_n^{(1)}\right\}$,

(ii) $W_2(z) := \sum_{n=1}^\infty \left\{|\langle\{C_{s,n}(z)\}_{n\in\mathbb{Z}}, \{\mathbf{e}_n^{(2)}\}_{n\in\mathbb{Z}}\rangle_{l^2}|^2/\sigma_n^{(2)}\right\}$,

(iii) $W_3(z) := \sum_{n=1}^\infty \left\{|\langle\{C_{p,n}(z)\}_{n\in\mathbb{Z}} \times \{C_{s,n}(z)\}_{n\in\mathbb{Z}}, \{\mathbf{e}_n^{(3)}\}_{n\in\mathbb{Z}}\rangle_{l^2}|^2/\sigma_n^{(3)}\right\}$.

The values of the indicator function $W_j(z)$ for z lying above the scattering surface should be relatively larger than those below the surface. In this way we establish the factorization method in elastic scattering by rigid surfaces, using the $k_p \sin\theta$-quasi-periodic incident elastic waves $u_{1,n}^{in}$. By the proof of Theorem 4.11, the parameter t entering into $N_{j\sharp}$ will be selected depending on the choice of the angle $\phi \in (0, \pi/2)$ given explicitly in the appendix.

Remark 4.12. In inverse acoustic scattering by diffraction gratings, the role of the positive coercive operator is usually played by the single-layer operator whose kernel is the quasi-periodic fundamental solution to the Helmholtz equation with the wavenumber $k = i$ or $k = 0$. This gives rise to an analogous inversion algorithm to Theorem 4.11 with the parameter $t = 0$. In the elastic case, more mathematical arguments would be involved in analyzing the D-to-N map and the middle operator when $\omega = i$ or $\omega = 0$. This is the reason why we turn to investigate properties of the middle operator with small frequencies as shown in Lemma 4.7 (i). However, our numerical experiments illustrate that the inversion algorithms with $t = 0$ still work well although a theoretical justification for that is not available yet.

The factorization method using $k_s \sin\theta$-quasi-periodic incident plane waves for the problems (**S**$_j$) can be established analogously.

Corollary 4.13. *Suppose*

(i) ω *is not a Dirichlet eigenvalue of the quasi-periodic Lamé operator in the periodic layer* Ω_0^- *with phase-shift* $\alpha = k_s \sin\theta$*,*

(ii) *either* $\sin^2\theta < \mu/(\lambda + 2\mu)$ *or* $|\sin\theta| > 1/2$ *holds.*

*Then, the results of Theorem 4.11 for (**P**$_j$) apply to the corresponding inverse problems (**S**$_j$),* $j = 1, 2, 3$.

Note that the second condition in Corollary 4.13 ensures the inequality (19) for $\alpha = k_s \sin\theta$; see Lemma A.1 (ii). Combining Theorem 4.11 and Corollary 4.13, we obtain the following uniqueness results for the inverse problem by utilizing only the compressional or shear part of the scattered field due to incident elastic waves with a common phase-shift. Define

$$\mathcal{I}(\alpha) := \{(\alpha_n, -\beta_n)^T \, \exp(i(\alpha_n x_1 - \beta_n x_2)) : n \in \mathbb{Z}\} \cup \{(\gamma_n, \alpha_n)^T \, \exp(i(\alpha_n x_1 - \gamma_n x_2)) : n \in \mathbb{Z}\}$$

Corollary 4.14. *Given an incident angle* $\theta \in (-\pi/2, \pi/2)$*. Under the conditions in Theorem 4.11 (resp. Corollary 4.13), a rigid diffraction grating surface can be uniquely determined from the knowledge of the compressional or shear part of the scattered field corresponding to each incoming wave from the set* $\mathcal{I}(\alpha)$ *with* $\alpha = k_p \sin\theta$ *(resp.* $\alpha = k_s \sin\theta$*).*

5 Numerical experiments

In this section we report numerical experiments to test the validity and accuracy of the factorization method for the inverse problems (**P**$_j$) and (**S**$_j$), $j = 1, 2, 3$. To generate the synthetic scattered data for downward incoming waves $u^{in}_{j,n,\mathsf{d}}(n \in \mathbb{Z})$ from the set $\mathcal{I}_j(\alpha)$, we solve an equivalent first-kind integral equation on Λ to (2) by using the discrete Galerkin method given in [14]. The n-th Rayleigh coefficients $A^{j,m}_{p,n}, A^{j,m}_{s,n}$ corresponding to the incident wave $u^{in}_{j,m}$ can be computed through the analysis at the end of Section 3. Define $(2M+1) \times (2M+1)$ matrix $N^{(M)}_{j,\tau}$:

$$N^{(M)}_{j,\tau} := \begin{pmatrix} A^{j,-M}_{\tau,-M} & A^{j,-M+1}_{\tau,-M} & \cdots & A^{j,0}_{\tau,-M} & \cdots & A^{j,M}_{\tau,-M} \\ A^{j,-M}_{\tau,-M+1} & A^{j,-M+1}_{\tau,-M+1} & \cdots & A^{j,0}_{\tau,-M+1} & \cdots & A^{j,M}_{\tau,-M+1} \\ \vdots & \vdots & \vdots & \vdots & \vdots & \vdots \\ A^{j,-M}_{\tau,M} & A^{j,-M+1}_{\tau,M} & \cdots & A^{j,0}_{\tau,M} & \cdots & A^{j,M}_{\tau,M} \end{pmatrix}, \quad j = 1, 2, \ \tau = p, s \qquad (27)$$

for some $M > 0$. Then the near-field operators N_j $(j = 1, 2)$ can be approximated by the matrices $N_1^{(M)} := N_{1,p}^{(M)}$ and $N_2^{(M)} := N_{2,s}^{(M)}$, respectively, whereas discretizing N_3 leads to the $(4N+2) \times (4N+2)$ matrix

$$N_3^{(M)} := \begin{pmatrix} N_{1,p}^{(M)} & N_{2,p}^{(M)} \\ N_{1,s}^{(M)} & N_{2,s}^{(M)} \end{pmatrix}$$

Let the singular value decomposition of $\mathrm{Re}\,[e^{i\phi} N^{(M)}]$ be given by

$$\mathrm{Re}\,(e^{i\phi} N^{(M)}) = V D V^{-1}$$

with D being the matrix of eigenvalues and V being the matrix of the corresponding eigenvectors of $\mathrm{Re}\,(e^{i\phi} N^{(M)})$. Then the operator $N_\sharp$ can be approximated by

$$N_\sharp^{(M)} = V D V^{-1} + \mathrm{Im}\,(N^{(M)})$$

Suppose we have the singular value decomposition of $N_\sharp^{(M)}$:

$$N_\sharp^{(M)} = U S U^{-1}$$

with S being the diagonal matrix of singular values σ_l and $U = (\psi_{n,l})$ being the matrix of the left singular vectors. Hence the Picard's range criterion can be approximated by the cut-off series

$$\begin{aligned}
\tilde{W}_1(z) &:= \Big[\sum_{l=1}^{2M+1} \frac{1}{\sigma_l} \Big| \sum_{n=-M}^{M} C_{p,n}(z) \overline{\psi}_{n+M+1,l} \Big|^2 \Big]^{-1/2}, \\
\tilde{W}_2(z) &:= \Big[\sum_{l=1}^{2M+1} \frac{1}{\sigma_l} \Big| \sum_{n=-M}^{M} C_{s,n}(z) \overline{\psi}_{n+M+1,l} \Big|^2 \Big]^{-1/2}, \\
\tilde{W}_3(z) &:= \Big[\sum_{l=1}^{4M+2} \frac{1}{\sigma_l} \Big| \sum_{n=-M}^{M} (C_{p,n}(z) \overline{\psi}_{n+M+1,l} + C_{s,n}(z)) \overline{\psi}_{n+M+2,l} \Big|^2 \Big]^{-1/2}
\end{aligned}$$

We will consider the following three grating profiles in our numerical experiments (see Figure 1):

(i) $f(x) = 0.6 + 0.5\sin(x), x \in (0, 2\pi)$, h = 1.3,

(ii) $f(x) = 0.5 + 0.3\sin(x) + 0.2\sin(2x), x \in (0, 2\pi)$, h = 1.2,

(iii) $f(x) = 0.2 + 0.2\exp(\sin(3x)) + 0.3\exp(\sin(4x)), x \in (0, 2\pi)$, h = 1.8.

In Figure 1 the red horizontal line indicates the detecting position Γ_h of our measurement for the scattered data.

Experiment 1: We apply the factorization method to the inverse problems $(\mathbf{P}_j)$ and $(\mathbf{S}_j), j = 1, 2, 3$ with fixed parameters $\omega = 5, \lambda = 1, \mu = 2, M = 30$ for distinct incident angles $\theta = \pi/6, \pi/3$. With these parameters we have the compressional wavenumber $k_p = \sqrt{5}$ and the shear wavenumber $k_s = 5/\sqrt{2}$, implying that most of our measurement data (Rayleigh coefficients) are from the surface waves with only

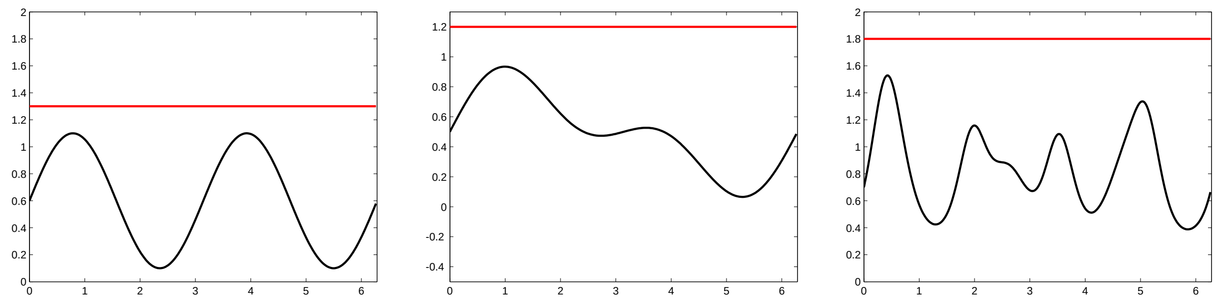

(a) Surface (i) (b) Surface (ii) (c) Surface (iii)

Figure 1: Test surfaces

a few from the propagating modes. We used unpolluted scattered near-field taken on Γ_h to reconstruct surfaces (i), (ii) and (iii). It can be seen from Figures 2, 3 and 4 that the factorization method gives satisfactory reconstructions particularly for mild surfaces (surface (i)), although poor reconstructions occur when the surface has deep grooves (e.g., surface (ii)) or oscillates heavily (e.g., surface (iii)). Evidently, using the entire near-field data gives better images than using only P-part or S-part data. In Figure 2, the reconstructions for ($\mathbf{P}_j$) and ($\mathbf{S}_j$) are nearly the same using different types of incident waves and Rayleigh coefficients, but those for ($\mathbf{P}_3$) and ($\mathbf{S}_3$) appear more reliable (see also Figures 3 and 4). However, in our settings it is not easy to conclude which one is superior by using P-part data and S-part data. The incident angles seem to have little effect on the quality of reconstructions.

Experiment 2: We take surface (ii) as an example to investigate the sensitivity of the factorization method to the noisy data. We only consider problems $(\mathbf{P}_j), j = 1, 2, 3$ for the incident angle $\theta = 0$ and take the other parameters as shown in Experiment 1. The Rayleigh coefficients are perturbed by the multiplication of $(1 + \delta\%\xi)$ with the noise level $\delta\%$, where ξ is an independent and uniformly distributed random variable generated between -1 and 1. Figure 5 illustrates the reconstructions from different noise levels at $\delta\% = 2\%, 5\%, 8\%$, respectively. It is seen that the factorization method with synthetic data is not very sensitive to the noise, and using the full near-field data seems more stable than using only compressional or shear waves.

Experiment 3: In the final experiment, we want to explore possible approaches to improve the reconstructions. At first, we consider the problem $(\mathbf{P}_1)$ for recovering surface (ii) with fixed $M = 30, \theta = 0$ and different incidence frequencies at $\omega = 5, 10, 20$. Figure 6 shows that higher frequency waves provide more accurate images than using lower frequencies. This can be explained by the fact that the number of propagating modes for $\omega = 20$ ($k_p \approx 8.9$) is much more than that for $\omega = 5$ ($k_p \approx 2.24$). The propagating wave modes contain more information of the scattering surface than the surface (evanescent) modes, because the latter propagates only along the grating profiles and decays exponentially in the x_2-direction. This is confirmed again in Figure 8 for recovering surface (iii) with different detecting positions. Since surface waves nearly cannot be measured at locations far away from the profiles, lowering the height of the measurement position contributes to better imaging quality. To see the effects of evanescent waves, we fix $\omega = 5$, $\theta = 0$ and compare the numerical results with different M. From Figure 7 we conclude that increasing the number of evanescent waves will enhance the imaging quality.

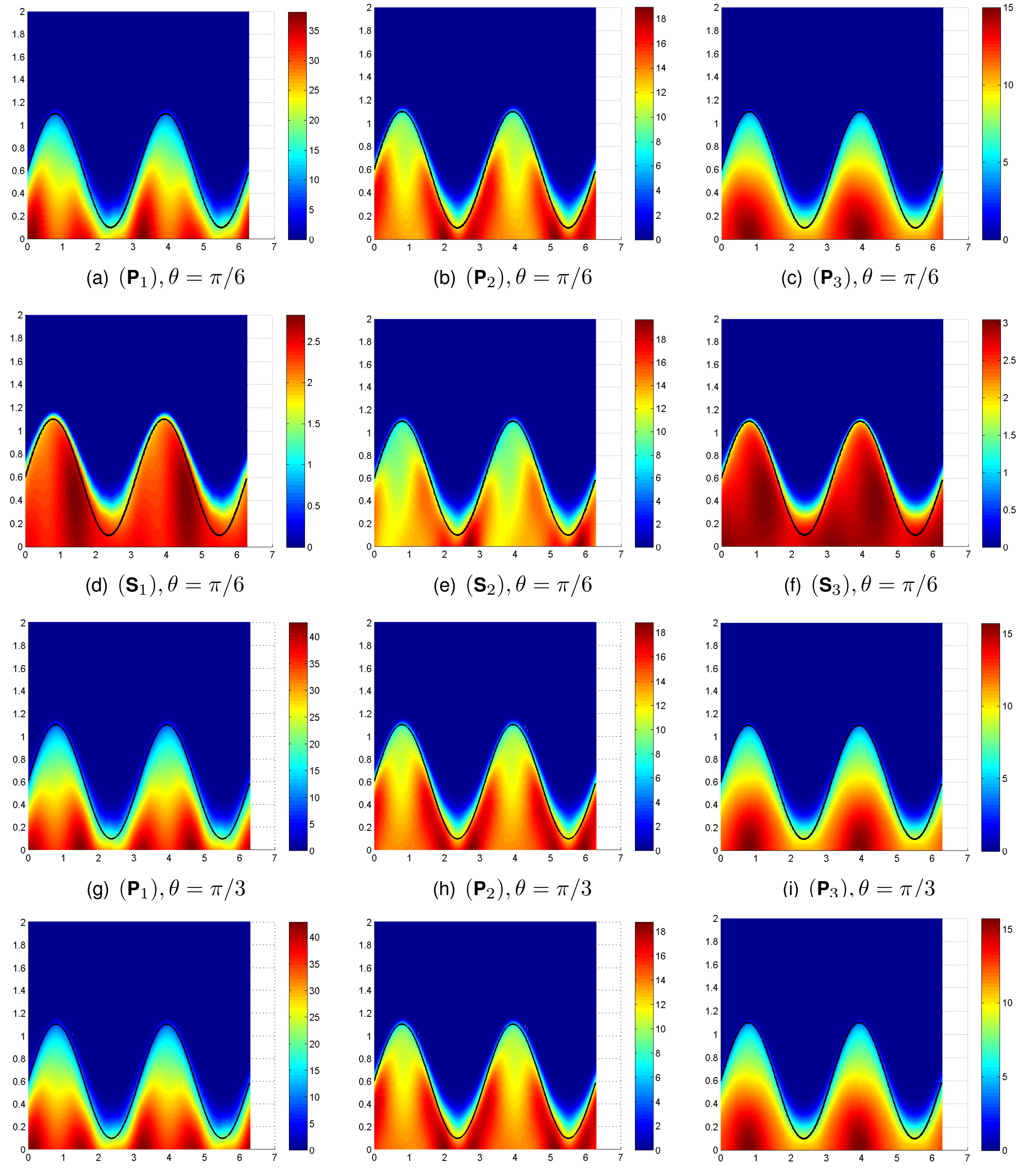

(a) $(\mathbf{P}_1), \theta = \pi/6$ (b) $(\mathbf{P}_2), \theta = \pi/6$ (c) $(\mathbf{P}_3), \theta = \pi/6$

(d) $(\mathbf{S}_1), \theta = \pi/6$ (e) $(\mathbf{S}_2), \theta = \pi/6$ (f) $(\mathbf{S}_3), \theta = \pi/6$

(g) $(\mathbf{P}_1), \theta = \pi/3$ (h) $(\mathbf{P}_2), \theta = \pi/3$ (i) $(\mathbf{P}_3), \theta = \pi/3$

(j) $(\mathbf{S}_1), \theta = \pi/3$ (k) $(\mathbf{S}_2), \theta = \pi/3$ (l) $(\mathbf{S}_3), \theta = \pi/3$

Figure 2: Experiment 1, surface (i)

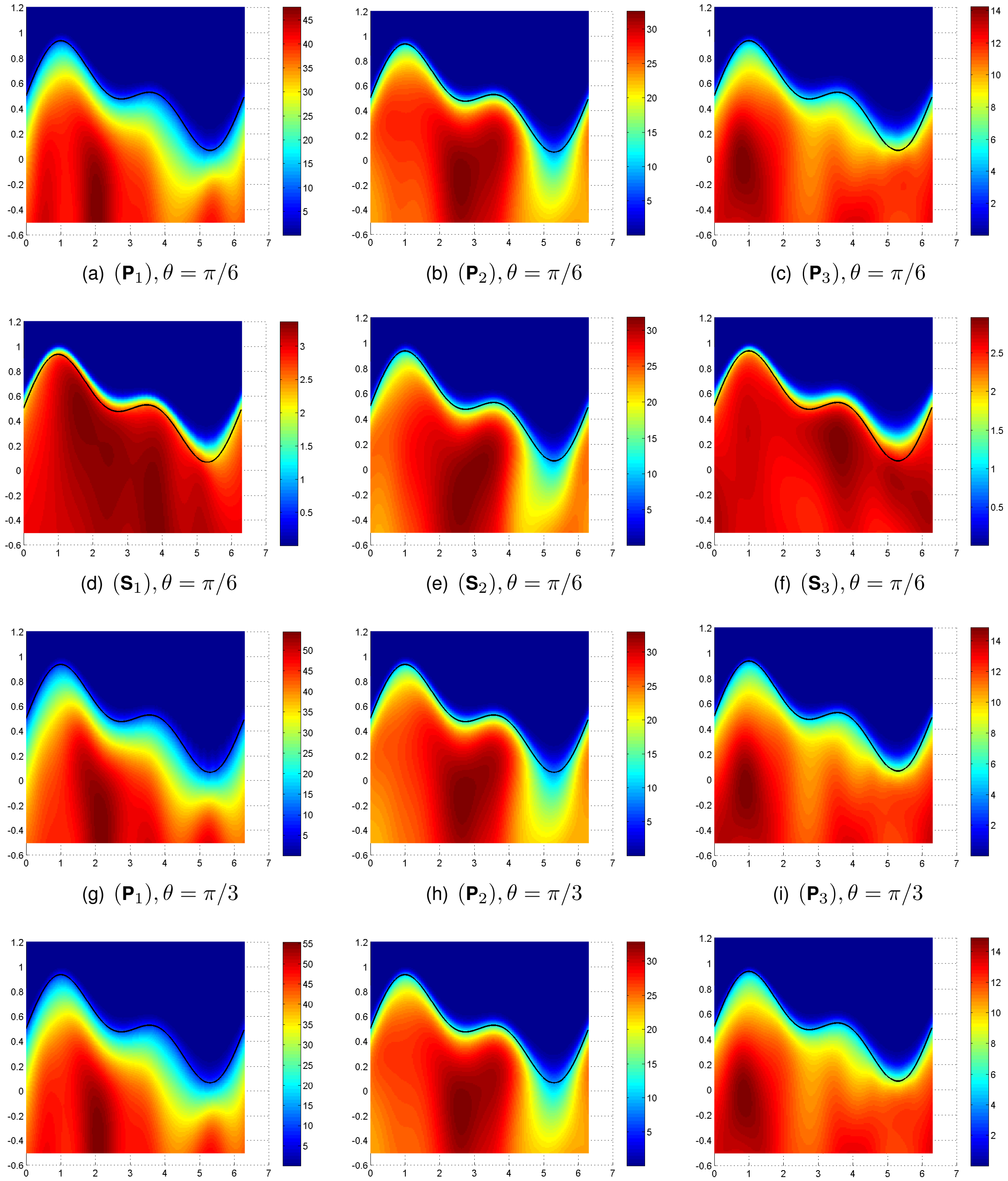

(a) $(\mathbf{P}_1), \theta = \pi/6$ (b) $(\mathbf{P}_2), \theta = \pi/6$ (c) $(\mathbf{P}_3), \theta = \pi/6$

(d) $(\mathbf{S}_1), \theta = \pi/6$ (e) $(\mathbf{S}_2), \theta = \pi/6$ (f) $(\mathbf{S}_3), \theta = \pi/6$

(g) $(\mathbf{P}_1), \theta = \pi/3$ (h) $(\mathbf{P}_2), \theta = \pi/3$ (i) $(\mathbf{P}_3), \theta = \pi/3$

(j) $(\mathbf{S}_1), \theta = \pi/3$ (k) $(\mathbf{S}_2), \theta = \pi/3$ (l) $(\mathbf{S}_3), \theta = \pi/3$

Figure 3: Experiment 1, surface (ii)

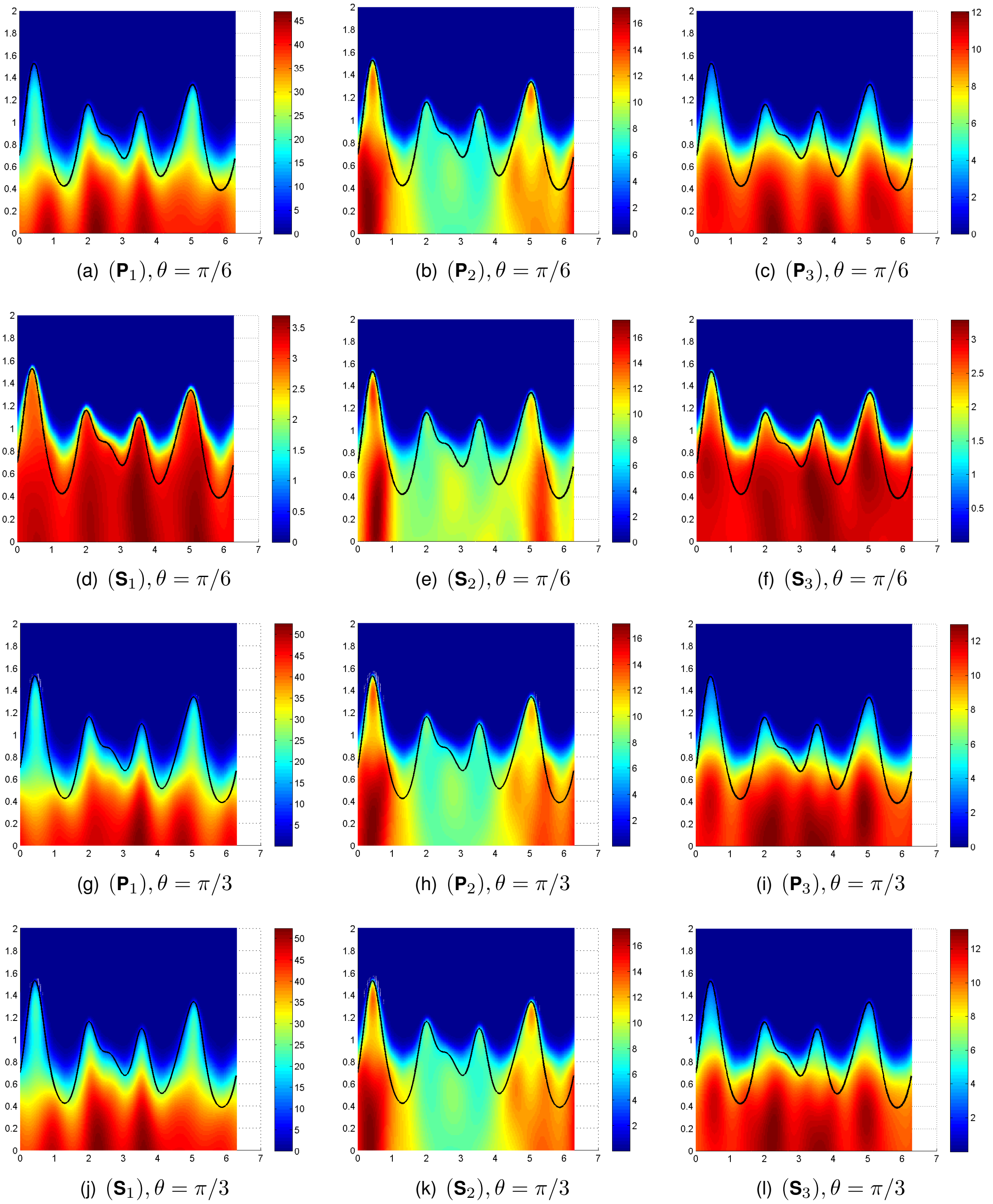

(a) $(\mathbf{P}_1), \theta = \pi/6$ (b) $(\mathbf{P}_2), \theta = \pi/6$ (c) $(\mathbf{P}_3), \theta = \pi/6$

(d) $(\mathbf{S}_1), \theta = \pi/6$ (e) $(\mathbf{S}_2), \theta = \pi/6$ (f) $(\mathbf{S}_3), \theta = \pi/6$

(g) $(\mathbf{P}_1), \theta = \pi/3$ (h) $(\mathbf{P}_2), \theta = \pi/3$ (i) $(\mathbf{P}_3), \theta = \pi/3$

(j) $(\mathbf{S}_1), \theta = \pi/3$ (k) $(\mathbf{S}_2), \theta = \pi/3$ (l) $(\mathbf{S}_3), \theta = \pi/3$

Figure 4: Experiment 1, surface (iii)

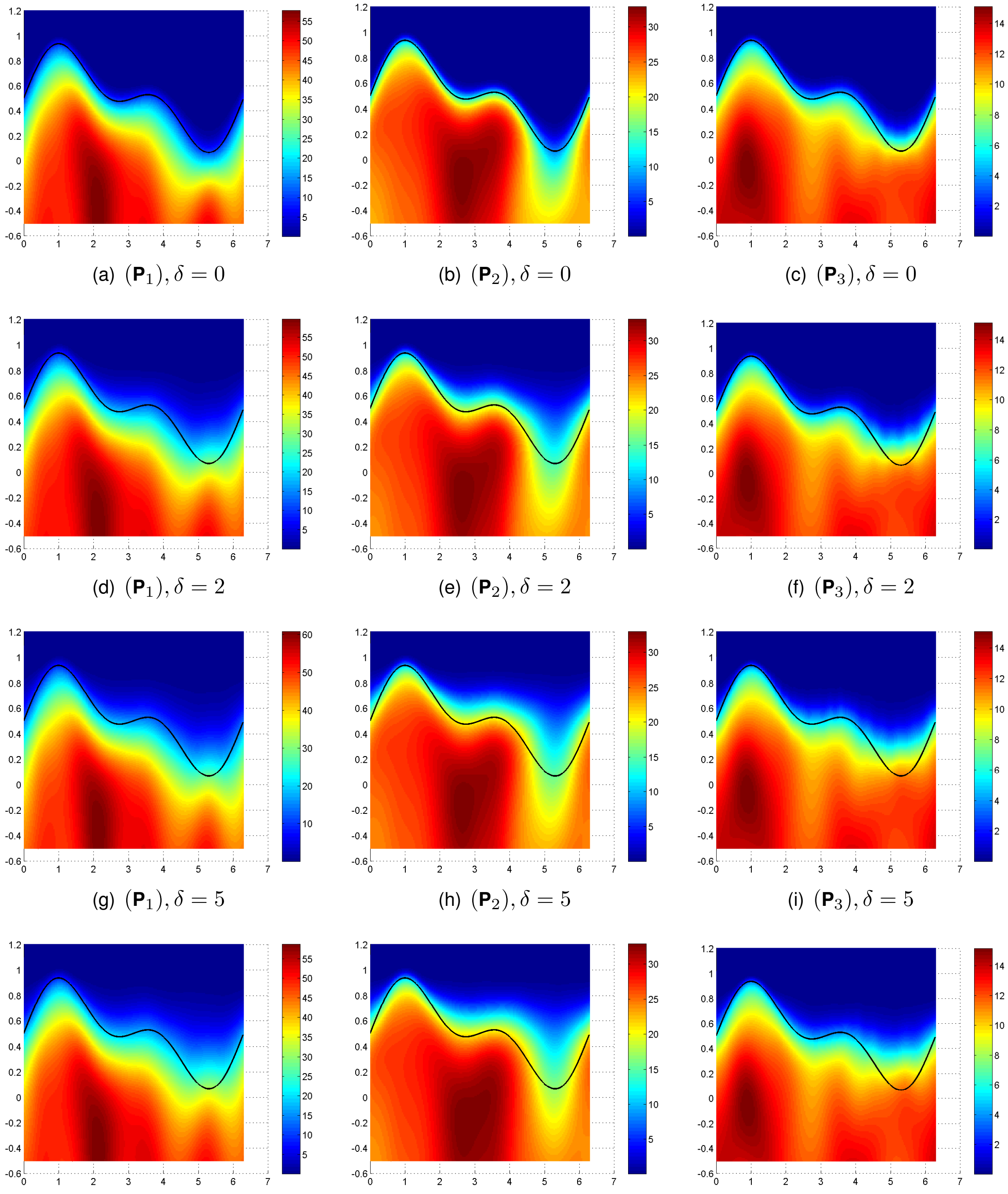

(a) $(\mathbf{P}_1), \delta = 0$ (b) $(\mathbf{P}_2), \delta = 0$ (c) $(\mathbf{P}_3), \delta = 0$

(d) $(\mathbf{P}_1), \delta = 2$ (e) $(\mathbf{P}_2), \delta = 2$ (f) $(\mathbf{P}_3), \delta = 2$

(g) $(\mathbf{P}_1), \delta = 5$ (h) $(\mathbf{P}_2), \delta = 5$ (i) $(\mathbf{P}_3), \delta = 5$

(j) $(\mathbf{P}_1), \delta = 8$ (k) $(\mathbf{P}_2), \delta = 8$ (l) $(\mathbf{P}_3), \delta = 8$

Figure 5: Experiment 2

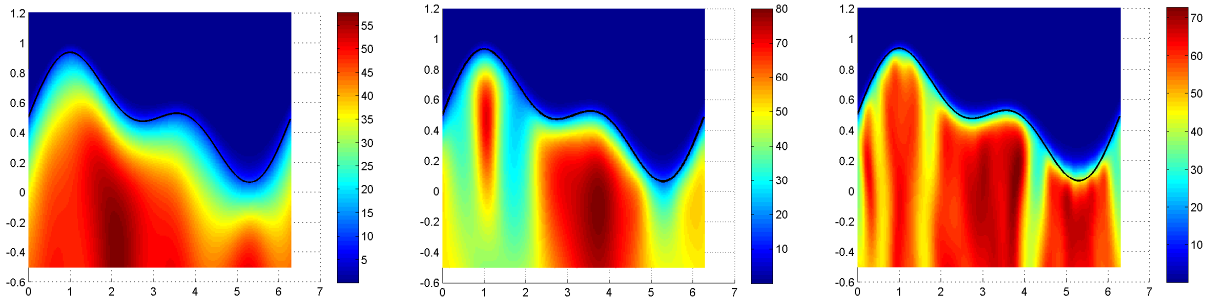

(a) $\omega = 5$ (b) $\omega = 10$ (c) $\omega = 20$

Figure 6: Experiment 3 for different ω. $\theta = 0, M = 30, h = 1.2$.

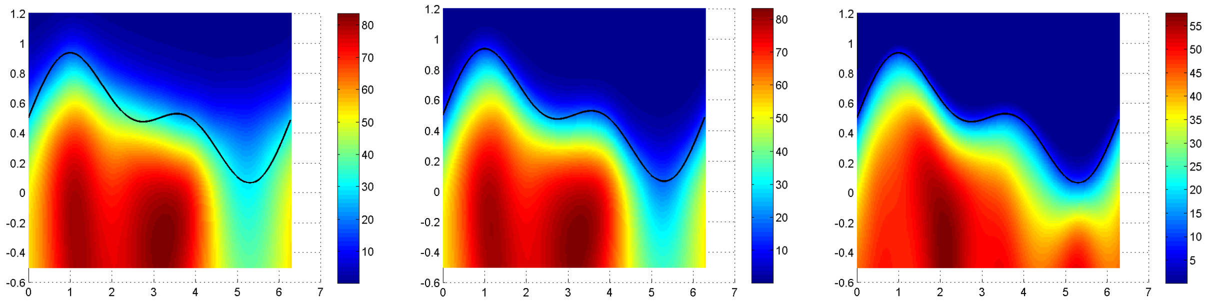

(a) $M = 5$ (b) $M = 15$ (c) $M = 30$

Figure 7: Experiment 3 for different M. $\omega = 5, \theta = 0, h = 1.2$.

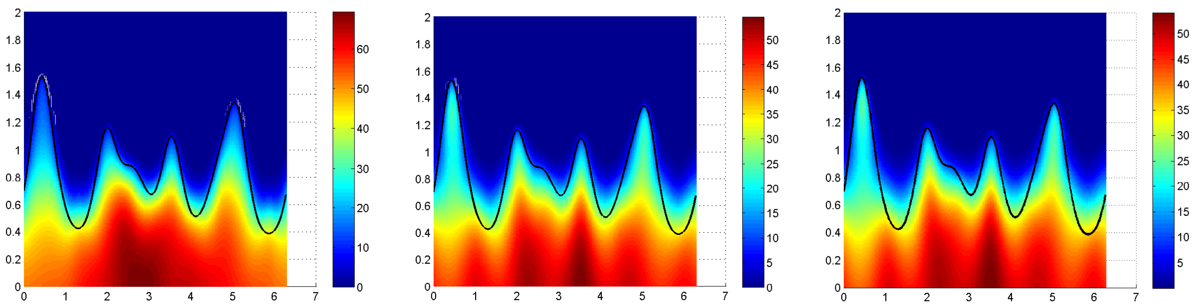

(a) $h = 1.6$ (b) $h = 1.8$ (c) $h = 2.0$

Figure 8: Experiment 3 for different h. $\omega = 5, \theta = 0, M = 30$.

Appendix

The following properties of the Dirichlet-to-Neumann (DtN) maps at small frequencies were used in the proof of Lemma 4.7 (i).

Lemma A.1. **(i)** *Let the Dirichlet-to-Neumann map $\mathcal{T}_\omega$ be given by* (20) *with $\alpha = k_p \sin\theta$. Then, there exist an angle $\phi \in (0, \pi/2)$ and a sufficiently small frequency $\omega_0 > 0$ such that*

$$-\mathrm{Re}\left\{\exp(i\phi)\int_{\Gamma_{\pm h}} \mathcal{T}_\omega u \cdot \overline{u}\, ds\right\} \geq c\,\omega\,\|u\|^2_{H^{1/2}_\alpha(\Gamma_{\pm h})^2}, \quad c > 0 \tag{A.1}$$

uniformly for $u \in H^{1/2}_\alpha(\Gamma_{\pm h})^2$ and $\omega \in (0, \omega_0]$.

(ii) *In the case $\alpha = k_s \sin\theta$, the first assertion remains valid provided either $\sin^2\theta < \mu/(\lambda + 2\mu)$ or $|\sin\theta| > 1/2$.*

Proof. (i) We prove (A.1) only for the DtN map defined on Γ_h. By the definition of $\mathcal{T}_\omega$, we have

$$-\int_{\Lambda_h} \mathcal{T}^+_\omega u \cdot \overline{u}\, ds = \sum_{n\in\mathbb{Z}} (M_{n,\omega} u_n, u_n)_{\mathbb{C}^2}, \quad \forall\, u \in H^{1/2}_\alpha(\Gamma_h)^2$$

where $\{u_n\}_{n\in\mathbb{Z}}$ stands for the Fourier coefficients of $\exp(-i\alpha)u|_{\Gamma_h}$. Thus it suffices to prove the existence of $\phi \in (0, \pi/2)$ and $\omega_0 > 0$ such that

$$\mathrm{Re}\big(\exp(i\phi)M_{n,\omega}\, z,\, z\big)_{\mathbb{C}^2} \geq c\,\omega\,(1 + |n|)\,|z|^2, \quad \text{for all} \quad \omega \in (0, \omega_0],\ n \in \mathbb{Z},\ z \in \mathbb{C}^2 \tag{A.2}$$

Observe that

$$\mathrm{Re}\big(\exp(i\phi)M_{n,\omega}\big) = \cos\phi\,\mathrm{Re}(M_{n,\omega}) - \sin\phi\,\mathrm{Im}(M_{n,\omega}) \tag{A.3}$$

and that for $\alpha = k_p \sin\theta$,

$$\{n : |\alpha_n| < k_p\} = \{0\}, \{n : |\alpha_n| > k_s\} = \{n : n \neq 0\}, \{n : k_p \leq |\alpha_n| \leq k_s\} = \varnothing \tag{A.4}$$

if $\omega \to 0$. For notational convenience we write (cf. 21)

$$M_{n,\omega} = \begin{pmatrix} ia_n & ic_n \\ -ic_n & ib_n \end{pmatrix}, \quad a_n = \frac{-\omega^2\beta_n}{t_n},\ b_n = \frac{-\omega^2\gamma_n}{t_n},\ c_n = \frac{\alpha_n}{t_n}(\omega^2 - 2\mu t_n) \tag{A.5}$$

We first prove (A.1) in the case $n \neq 0$. Elementary calculation shows that

$$t_n = \alpha_n^2 - \sqrt{\alpha_n^2 - k_p^2}\sqrt{\alpha_n^2 - k_s^2} = \frac{k_p^2 + k_s^2}{2} + \mathcal{O}(\omega^4) \quad \text{as } \omega \to 0 \tag{A.6}$$

Combining (A.4) and (A.6) then yields

$$\begin{aligned} &ia_n = -i\omega^2\beta_n/t_n \geq c_1\omega(1 + |n|) > 0, \quad \mathrm{Im}\, M_{n,\omega} = 0, \\ &\det(\mathrm{Re}\, M_{n,\omega}) = (4\alpha_n^2\mu(\omega^2 - \mu t_n) - \omega^4)/t_n \geq c_2\,\omega^2(1 + |n|)^2 > 0 \end{aligned} \tag{A.7}$$

as $\omega \to 0$, with some constants $c_1, c_2 > 0$ independent of u and ω. The estimate (A.2) then follows from (A.7) and (A.3) for all $\phi \in (0, \pi/2)$ and $n \neq 0$.

We next consider the case $n = 0$, which implies that $a_0, b_0, c_0, t_0 \in \mathbb{R}$,

$$\mathrm{Re}(M_{0,\omega}) = \begin{pmatrix} 0 & ic_0 \\ -ic_0 & 0 \end{pmatrix}, \quad \mathrm{Im}(M_{0,\omega}) = \begin{pmatrix} a_0 & 0 \\ 0 & b_0 \end{pmatrix}$$

Consequently,

$$\mathrm{Re}\big(\exp(i\phi)M_{0,\omega}\big) = \begin{pmatrix} -a_0\sin\phi & ic_0\cos\phi \\ -ic_0\cos\phi & -b_0\sin\phi \end{pmatrix}$$

Moreover, the $(1,1)$-th entry and the determinant of the above matrix can be more precisely reformulated in terms of λ, μ, ω and ϕ as

$$\begin{aligned} -a_0\sin\phi &= \omega\sqrt{2\mu+\lambda}\cos\theta\sin\phi/H_0(\theta,\lambda,\mu), \\ \mathrm{det}[\mathrm{Re}\big(\exp(i\phi)M_{0,\omega}\big)] &= \omega^2(2\mu+\lambda)(\tan^2\phi - H_1(\theta,\lambda,\mu))/H_0^2(\theta,\lambda,\mu) \end{aligned}$$

where

$$\begin{aligned} H_0(\theta,\lambda,\mu) &:= \sin^2\theta + \cos\theta\sqrt{(2\mu+\lambda)/\mu - \sin^2\theta} > 0, \\ H_1(\theta,\lambda,\mu) &:= \frac{\sin^2\theta\left[1 - 2\mu(\frac{\sin^2\theta}{2\mu+\lambda} + \frac{1}{\sqrt{2\mu+\lambda}}\cos\theta\sqrt{\frac{1}{\mu} - \frac{\sin^2\theta}{2\mu+\lambda}})\right]^2}{\cos\theta\sqrt{(2\mu+\lambda)/\mu - \sin^2\theta}} \geq 0 \end{aligned}$$

Taking $\phi \in (0, \pi/2)$ such that $\tan^2\phi > H_1(\theta,\lambda,\mu)$, we get

$$-a_0\sin\phi \geq c\,\omega, \quad \mathrm{det}[\mathrm{Re}\big(\exp(i\phi)M_{0,\omega}\big)] \geq c\omega^2, \quad \forall\,\omega \in (0,\omega_0]$$

for some constant $c > 0$ independent of $\omega \in (0,\omega_0]$. From this the estimate (A.1) follows when $n = 0$. The first assertion is thus proven.

(ii) Let $\alpha = k_s\sin\theta$. If $\sin^2\theta < \mu/(\lambda+2\mu)$ (or equivalently $k_p^2 > k_s^2\sin^2\theta$), then the relations in (A.4) remain valid for small ω. Hence, repeating the same arguments in proving (i) gives the estimate (A.1) for this case. Next, under the assumption that $\sin^2\theta \geq \mu/(\lambda+2\mu)$ and $\sin^2\theta > 1/4$ we will verify the estimate (A.2) by arguing similarly as in (i).

For $n \neq 0$ and small ω, we have $\beta_n = i|\beta_n|, \gamma_n = i|\gamma_n|$ and $t_n = \alpha_n^2 - |\beta_n||\gamma_n|$ if $\sin^2\theta \geq \mu/(\lambda+2\mu)$. Consequently, by (A.5) we have $\mathrm{Im}\,(M_{n,\omega}) = 0$ and $(\mathrm{Re}\,(M_{n,\omega})z, z) \geq c\,\omega|n||z|^2$ for $z \in \mathbb{C}^2$, $n \neq 0$, $\omega \in (0,\omega_0]$. Therefore, for any $\phi \in (0,\pi/2)$ one can verify the inequality (A.2) again whenever $n \neq 0$.

Additional arguments are needed in the case $n = 0$, for which we have $\beta_0 = i|\beta|, \gamma_0 = \gamma, t_0 = \alpha^2 + i|\beta|\gamma$ and

$$M_{0,\omega} = \frac{i}{t_0}N_0, \quad N_0 := \begin{pmatrix} -i\omega^2\beta & c_0 \\ -c_0 & -\omega^2\gamma \end{pmatrix}, \quad c_0 = \alpha(\omega^2 - 2\mu t_0)$$

By elementary calculations, the matrix $\mathrm{Re}\,(e^{i\phi}M_{0,\omega})$ takes the form

$$\mathrm{Re}\,(e^{i\phi}M_{0,\omega}) = \frac{\cos\phi}{\alpha^4 + |\beta|^2\gamma^2}\,\tilde{N}_{0,\omega}, \quad \tilde{N}_{0,\omega} := \begin{pmatrix} (\alpha^2 + \tan\phi|\beta|\gamma)\omega^2|\beta| & id \\ -id & (\tan\phi\alpha^2 - |\beta|\gamma)\omega^2\gamma \end{pmatrix}$$

where $d = (\tan\phi\alpha^2 - |\beta|\gamma)2\mu\alpha|\beta|\gamma + (\alpha^2 + \tan\phi|\beta|\gamma)\alpha(\omega^2 - 2\mu\alpha^2)$. For small ω, the $(1,1)$-th entry of the matrix $\tilde{N}_{0,\omega}$ is bounded below:

$$(\alpha^2 + \tan\phi|\beta|\gamma)\omega^2|\beta| \geq c_1\,\omega^5, \quad \forall\,\phi \in (0, \pi/2), \quad c_1 = c_1(\phi) > 0$$

The determinant of $\tilde{N}_{0,\omega}$ can be written as det$(\tilde{N}_{0,\omega}) = \tan\phi\, I_1(\theta, \lambda, \mu, \omega) - I_2(\theta, \lambda, \mu, \omega)$, where

$$\begin{aligned} I_1 &= (\alpha^2 + |\beta|^2\gamma^2)|\beta|\gamma(4\sin^2\theta - 1)\omega^2, \\ I_2 &= \left(\alpha^3(\omega^2 - 2\mu\alpha^2) - 2\mu\alpha|\beta|^2\gamma^2\right)^2 + \omega^4|\beta|^2\gamma^2\alpha^2 > 0 \end{aligned}$$

Obviously, $I_1 > 0$ if $|\sin\theta| > 1/2$. Now, choosing $\phi \in (0, \pi/2)$ such that $\tan\phi > I_2/I_1 > 0$, we deduce that det$(\tilde{N}_{0,\omega}) \geq c_2\,\omega^6$ as $\omega \to 0$ for some constant $c_2 = c_2(\phi) > 0$. Finally, making use of the asymptotic behavior $\alpha^4 + |\beta|^2\gamma^2 \sim \omega^4$ as $\omega \to 0$, we obtain (A.2) for $n = 0$ in the case when $\sin^2\theta \geq \mu/(\lambda + 2\mu)$ and $\sin^2\theta > 1/4$. Note that det$(\tilde{N}_{0,\omega}) < 0$, so the matrix $\mathrm{Re}\,(e^{i\phi}\,M_{0,\omega})$ is not definite when $|\sin\theta| < 1/2$. $\square$

References

[1] Ammari H 1995 Uniqueness theorems for an inverse problem in a doubly periodic structures *Inverse Problems* **11** 823-833

[2] Alves C J and Kress R 2002 On the far-field operator in elastic obstacle scattering, *IMA J. Appl. Math.* **67** 1-21

[3] Arens T 1999 The scattering of plane elastic waves by a one-dimensional periodic surface, *Math. Meth. Appl. Sci.* **22** 55-72

[4] Arens T 1999 A new integral equation formulation for the scattering of plane elastic waves by diffraction gratings, *J. Int. Equ. Appl.* **11** 275–297

[5] Arens T and Grinberg N 2005 A complete factorization method for scattering by periodic surface, *Computing* **75** 111-132

[6] Arens T and Kirsch A 2003 The factorization method in inverse scattering from periodic structures, *Inverse Problems* **19** 1195-1211

[7] Bao G, Cowsar L and Masters W (eds.) 2001 *Mathematical Modeling in Optical Science*, Philadelphia, USA: SIAM

[8] Bonnet-Bendhia A S and Starling P 1994 Guided waves by electromagnetic gratings and non-uniqueness examples for the diffraction problem, *Math. Meth. Appl. Sci.* **17** 305–338

[9] Chandler-Wilde S N and Elschner J 2012 Variational approach in weighted Sobolev spaces to scattering by unbounded rough surfaces, *SIAM J. Math. Anal.* **42** 2554–2580

[10] Charalambopoulos A, Gintides D and and Kiriaki K 2001 On the uniqueness of the inverse elastic scattering problem for periodic structures, *Inverse Problems* **17** 1923-1935

[11] Charalambopoulos A, Kirsch A, Anagnostopoulos K A, Gintides D and Kiriaki K 2007 The factorization method in inverse elastic scattering from penetrable bodies, *Inverse Problems* **23** 27-51

[12] Elschner J and Hu G 2010 Variational approach to scattering of plane elastic waves by diffraction gratings *Math. Meth. Appl. Sci.* **33** 1924-1941

[13] Elschner J and Hu G 2012 Scattering of plane elastic waves by three-dimensional diffraction gratings, *Math. Models Methods Appl. Sci.* **22** 1150019

[14] Elschner J and Hu G 2012 An optimization method in inverse elastic scattering for one-dimensional grating profiles, *Commun. Comput. Phys* **12** 1432-1460

[15] Elschner J and Hu G 2013 Elastic scattering by unbounded rough surfaces: solvability in weighted Sobolev spaces, *WIAS Preprint* **1780**

[16] Elschner J, Hsiao G C and Rathsfeld A 2003 Grating profile reconstruction based on finite elements and optimization techniques, *SIAM J. Appl. Math.* **64** 525-545

[17] Fokkema J T 1980 Reflection and transmission of elastic waves by the spatially periodic interface between two solids (theory of the integral-equation method), *Wave Motion* **2** 375-393

[18] Fokkema J T and Van den Berg P M 1977 Elastodynamic diffraction by a periodic rough surface (stress-free boundary), *J. Acoust. Soc. Am.* **62** (5) 1095-1101

[19] Hettlich F 2002 Iterative regularization schemes in inverse scattering by periodic structures, *Inverse Problems* **18** 701-714

[20] Hettlich F and Kirsch A 1997 Schiffer's theorem in inverse scattering for periodic structures, *Inverse Problems* **13** 351-361

[21] Hu G, Kirsch A and Sini M 2013 Some inverse problems arising from elastic scattering by rigid obstacles, *Inverse Problems* **29** 015009

[22] Ito K and Reitich F 1999 A high-order perturbation approach to profile reconstruction: I. Perfectly conducting grating, *Inverse Problems* **15** 1067-1085

[23] Kirsch A 1993 Diffraction by periodic structures In: *L. Päivärinta et al, editors, Proc. Lapland Conf. Inverse Problems* (Berlin: Springer) 87-102

[24] Kirsch A 1998 Characterization of the shape of a scattering obstacle using the spectral data of the far field operator, *Inverse Problems* **14** 1489-1512

[25] Kirsch A 2004 The factorization method for Maxwell's equations, *Inverse Problems* **20** S117-S134

[26] Kirsch A and Grinberg N 2008 *The Factorization Method for Inverse Problems*, Oxford Univ. Press.

[27] Linton C M 1998 The Green's function for the two-dimensional Helmholtz equation in periodic domains, *J. Eng. Math* **33** 377-401

[28] Lechleiter A 2008 *Factorization Methods for Photonics and Rough Surfaces*, PhD thesis, University of Karlsruhe, Karlsruhe, Germany

[29] Nakagawa S, Nihei K T, Myer L R and Majer E L 2003 Three-dimensional elastic wave scattering by a layer containing vertical periodic fractures *J. Acoust. Soc. Am.* **113** 3012-3023

[30] Nguyen D L 2012 *Spectral Methods for Direct and Inverse Scattering from Periodic Structures*, PhD thesis, Ecole Polytechnique, Palaiseau, France

[31] Sandfort K 2010 *The Factorization Method for Inverse Scattering from Periodic Inhomogeneous Media*, PhD thesis, University of Karlsruhe, Karlsruhe, Germany

[32] Turunen J and Wyrowski F (eds) 1997 *Diffractive Optics for Industrial and Commercial Applications* (Berlin: Akademie)

[33] Yang J, Zhang B and Zhang R 2012 A sampling method for the inverse transmission problem for periodic media, *Inverse Problems* **28** 035004

[34] Yang J, Zhang B and Zhang R 2012 Reconstruction of penetrable gratings, Submitted